NOAA Pacific Marine Environmental Laboratory
Ocean Climate Stations Project

# DATA ACQUISITION AND PROCESSING REPORT FOR KE016

| | |
|---|---|
| *Site Name:* | Kuroshio Extension Observatory (KEO) |
| ***Deployment Number:*** | **KE016** |
| *Year Established:* | 2004 |
| *Nominal Location:* | 32.3°N 144.6°E |
| *Anchor Position:* | 32° 23.02' N 144° 32.41' E (triangulated) |
| *Deployment Date:* | July 3rd, 2018 |
| *Recovery Date:* | September 26th, 2019 |
| *Project P.I.:* | Dr. Meghan F. Cronin |
| *Report Authors:* | N.D. Anderson, P. Berk, M.F. Cronin |
| *Data Processors:* | N.D. Anderson |
| *Date of Report:* | January 18, 2023 |
| *Revision History:* | October 11, 2019 (initial draft) |

# Table of Contents



## List of Tables

## List of Figures

# Data Acquisition and Processing Report for OCS Mooring KE016

## 1.0 Mooring Summary

The NOAA Ocean Climate Stations reference mooring at the Kuroshio Extension Observatory (KEO) site was established with the deployment of the KE001 mooring in June 2004. The 2004 deployment was part of the first year of the two-year Kuroshio Extension System Study (KESS). At the conclusion of KESS, a partnership with the Japan Agency for Marine-Earth Science and Technology (JAMSTEC) was formed.

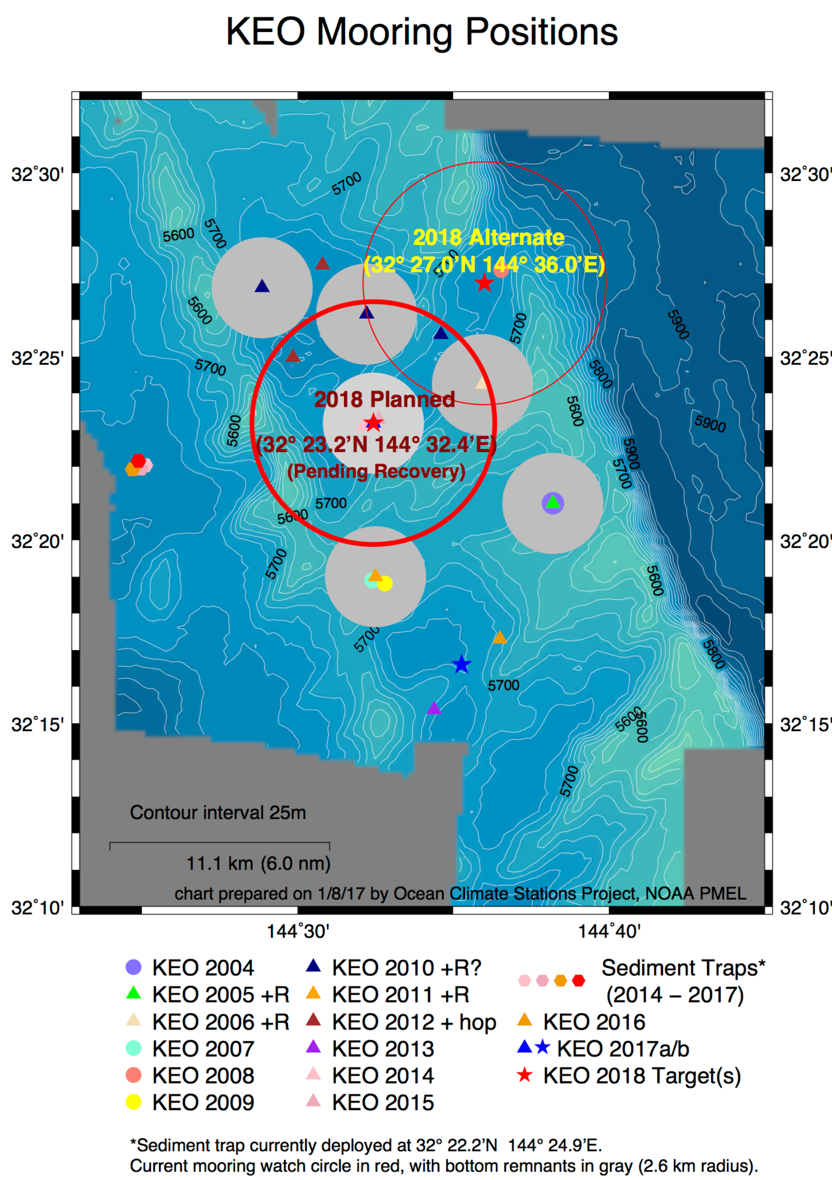


**Figure 1: KEO regional map, with the KE016 position and JAMSTEC sediment trap at the time of deployment.**

KE016 was the 15th deployment at the KEO site (the KE004 name was given to a buoy deployed at the nearby JKEO site, maintained by JAMSTEC). The mooring was deployed on July 3rd, 2018 by the M/V BLUEFIN, and recovered September 26th, 2019 by the M/V KAIYO MARU #1. The captain and crew of both ships are gratefully acknowledged for their support in maintaining long-term observations at this reference station.

Because the previous mooring had gone adrift and was redeployed, Figure 1 shows two positions for KEO 2017, signifying a) the position of the bottom remnant and b) the 2017 redeployment. The planned deployment location for the 2018 mooring matched 2017a, and was utilized after the successful remnant recovery at that location. The alternate deployment location for 2018 went unused, having been reserved as backup in case the remnant recovery failed.

KE016 witnessed the close passage of typhoons Jongdari and Shanshan. Both exhibited a characteristic decrease in atmospheric pressure and increase in winds, with decreased sensor depths (and steeper line angles) as the buoy was pulled to the edge of its watch circle. Typhoon Tapah (September 2019) delayed recovery efforts, but mooring operations proceeded on September 26th after the typhoon passed the Yokohama region to the north and west. Weather conditions during recovery required technicians to hook the buoy from the starboard side of the ship, where contact with the hull damaged both wind sensors and a shortwave radiometer's shield.

## 1.1 Mooring Description

The KE016 mooring was a slack-line mooring, with a nominal scope of 1.4. Non-rotating 7/16" (1.11cm) diameter wire rope, jacketed to 1/2" (1.27cm), was used in the upper 700m of the mooring line. Plastic fairings were installed on the wire rope from 1m – 150m and 240m – 350m. The remainder of the mooring line consisted of plaited 8-strand nylon line, spliced to buoyant polyolefin, as shown in Figure 3. There were 18 glass balls in line above the acoustic release. The 8,240lb (3,738kg) anchor was fabricated from scrap railroad wheels.

The upper portion of the mooring was kept fairly vertical by using a reverse catenary design, but less so than with taut-line moorings. Since instrument depths change on a slack line mooring, most KEO instruments measure pressure. Interpolated pressures are used in salinity calculations where no pressure measurements exist.

The surface buoy was a 2.6m fiberglass-over-foam discus buoy, with a central instrument well. It had an aluminum tower and a stainless steel bridle.

**Figure 2: KE016 as deployed.**

OCS partner groups also provided mooring instrumentation. The PMEL carbon group (PI: Dr. Adrienne Sutton) contributed an SBE16 package (with an attached oxygen sensor and fluorometer) and a Sami pH sensor mounted on the buoy bridle, along with their primary $CO_2$ flux monitoring system housed in the buoy well. A passive acoustic listening device (PAL) from Dr. Jie Yang of the University of Washington Applied Physics Lab (UW/APL) was deployed at 500m with a redesigned mounting bracket, and was recovered successfully for the first time. OCS is not responsible for the acquisition or processing of these data, and no further discussion of these systems are included in this report. All OCS and partner systems with corresponding instrumentation are shown in the mooring diagram (Figure 3).

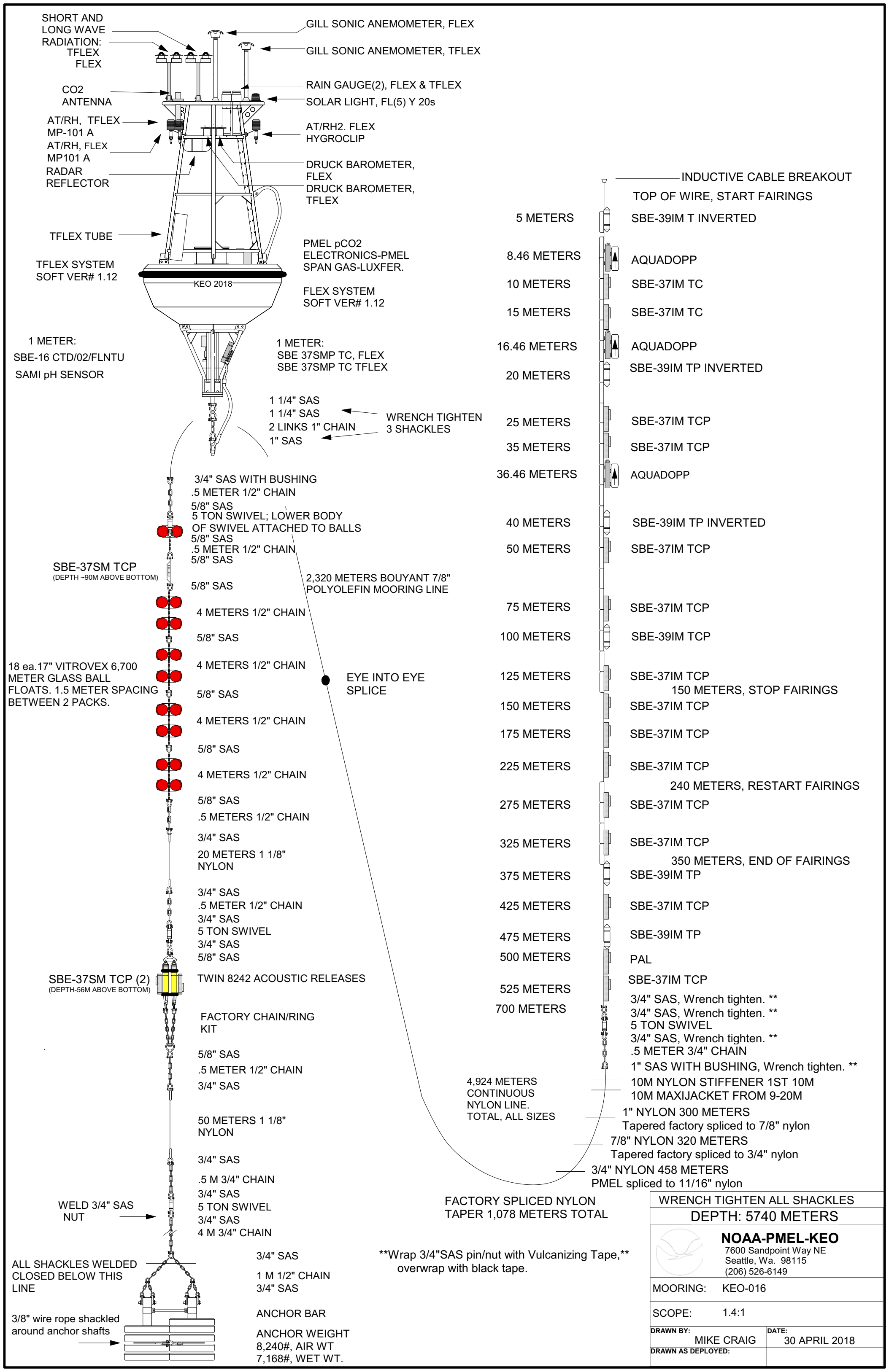


**Figure 3: KE016 mooring diagram.**

## 1.2 Instrumentation on KE016

The following instrumentation was deployed on KE016. Redundant data acquisition systems were used, Flex and TFlex. Flex meteorological sensors are generally considered primary. Any substitutions are noted in the relevant section of this report.

| **Deployment:** | | **KE016** | | | |
|---|---|---|---|---|---|
| **Met Sensors** | | **Model** | **Serial #** | | **Notes** |
| **Height** | Acquisition | **FLEX** | 6 | | |
| 2.6m | ATRH | Rotronics MP-101A | 133403 | | |
| 2.6m | ATRH2 | Rotronics HygroClip | 20086871 | | |
| 4.2m | Wind | Gill | 073805 | | |
| 2.5m | BP | Druck | 4299622 | | |
| 3.1m | Rain | RM Young | 1628 | | |
| 3.6m | SWR | Eppley PSP | 38429 | | |
| 3.6m | LWR | Eppley PIR | 38488 | | |
| | Acquisition | **TFLEX** | 2004 | | |
| 2.6m | ATRH | Rotronics MP-101A | 461007 | | |
| 3.8m | Wind | Gill | 14180061 | | |
| 2.5m | BP | Druck | 4253762 | | |
| 3.1m | Rain | RM Young | 1811 | | |
| 3.6m | SWR | Eppley PSP | 38432 | | |
| 3.6m | LWR | Eppley PIR | 38692 | | |
| | | | | | |
| **CO2** | Electronics | PMEL | 0013 | | |
| | Span Gas | Luxfer | | | |
| | | | | | |
| **Subsurface Instrumentation** | | | | | |
| **Bridle** | | **Model** | **Serial #** | | **Notes** |
| 1m | SST/C | SBE37SMP - TC | 12520 | | Flex, AA |
| 1m | SST/C | SBE37SMP - TC | 11552 | | TFLEX |
| 1m | pH | Sami | P0082 | | CO2 |
| 1m | SST/C | SBE16+V2 | 6885 | | CO2 |
| 1m | Oxygen | Optode | 1571 | | Attached to CO2 SBE16+ |
| 1m | Fluorescence | ECO FLNTUS | 2852 | | Attached to CO2 SBE16+ |
| | | | | | |
| **Depth** | | **Model** | **Serial #** | **IM ID** | **Notes** |
| 5m | T | SBE39IM-T | 3283 | 01 | |
| 8.46m | ADCM | AquaDopp | 12026 | 02 | |
| 10m | TC | SBE37IM - TC | 7793 | 03 | |
| 15m | TC | SBE37IM - TC | 9412 | 04 | |
| 16.46m | ADCM | AquaDopp | 6290 | 05 | |
| 20m | TP | SBE39IM-TP | 4861 | 06 | |
| 25m | TCP | SBE37IM - TCP | 7103 | 07 | |
| 35m | TCP | SBE37IM - TCP | 7104 | 08 | |
| 36.46m | ADCM | AquaDopp | 6808 | 09 | |
| 40m | TP | SBE39IM-TP | 4857 | 10 | |
| 50m | TCP | SBE37IM - TCP | 7105 | 11 | |
| 75m | TCP | SBE37IM - TCP | 7106 | 12 | |
| 100m | TCP | SBE37IM - TCP | 7107 | 13 | |
| 125m | TCP | SBE37IM - TCP | 7108 | 14 | |
| 150m | TCP | SBE37IM - TCP | 9413 | 15 | |
| 175m | TCP | SBE37IM - TCP | 7781 | 16 | |
| 225m | TCP | SBE37IM - TCP | 7782 | 17 | |
| 275m | TCP | SBE37IM - TCP | 7783 | 18 | |
| 325m | TCP | SBE37IM - TCP | 7784 | 19 | |
| 375m | TP | SBE39IM-TP | 4360 | 20 | |
| 425m | TCP | SBE37IM - TCP | 7780 | 21 | |
| 475m | TP | SBE39IM-TP | 4378 | 22 | |
| 500m | PAL | PAL | XANTUS | | UW- New depth |
| 525m | TCP | SBE37IM - TCP | 7092 | 23 | |
| 700m | End of Wire | | | | |
| | | | | | |
| Glass Balls | TCP | SBE37SM - TCP | 12243 | | OceanSITES loaner |
| Release | TCP | SBE37SM - TCP | 11926 | - | OCS |
| Release | TCP | SBE37SM - TCP | 11456 | | SBE Loaner. Pumped |

**Table 1: Instruments deployed on KE016.**

Since 2007, the measurement point for bridle sensors, including the SST/C, is known to have varied between 1.0 - 1.3m depth. Uncertainties in actual measurement depth are introduced by changes in buoy waterlines, variation between instrument mounting locations, and alteration of measurement points with different instrument versions. For these reasons, the nominal depth for all bridle sensors is stated as 1m.

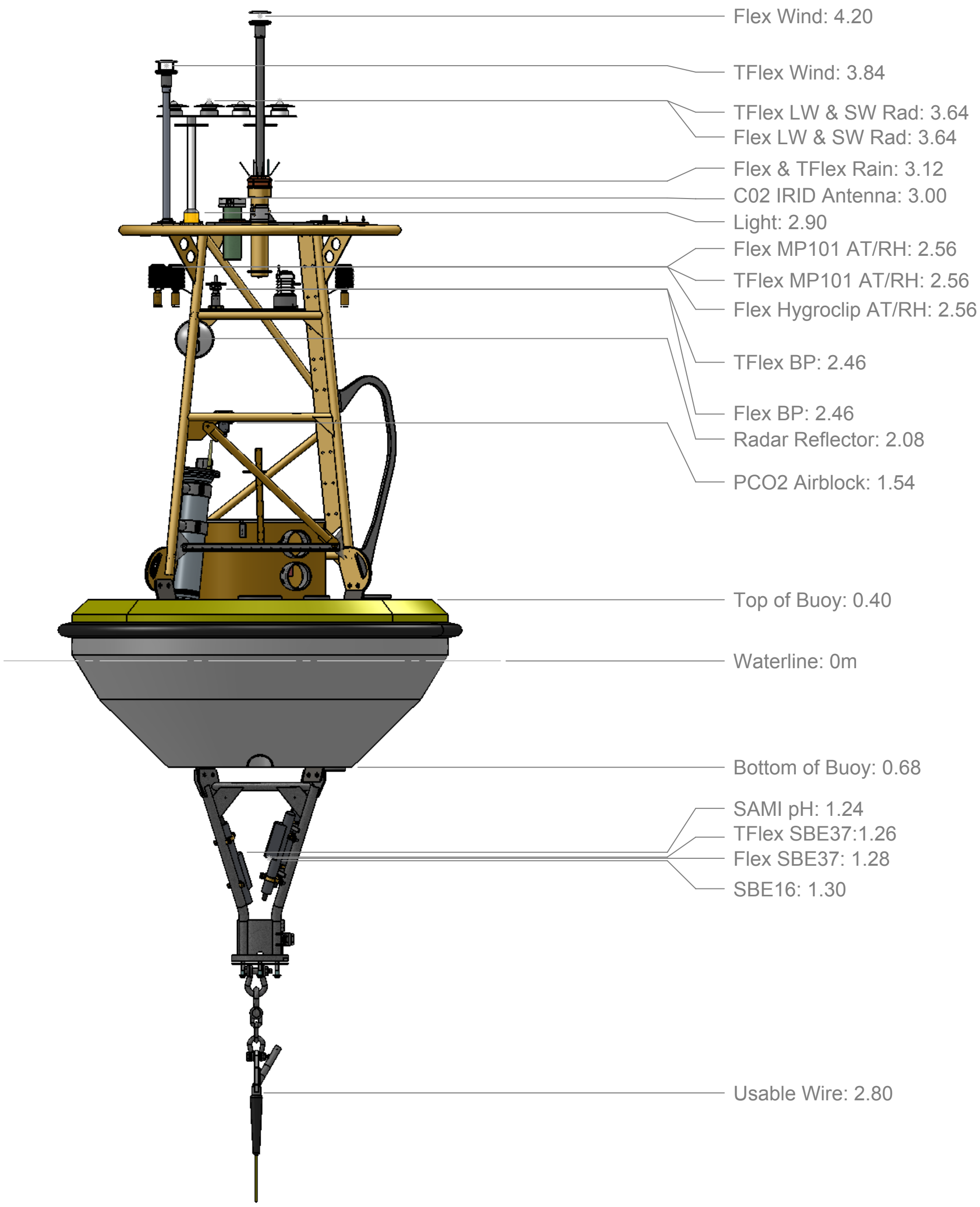


**Figure 4: Buoy diagram showing bridle arrangement. The SBE16 package contains a suite of sensors.**

# 2.0 Data Acquisition

Two independent data acquisition systems were deployed on KE016, Flex and TFlex. Both systems telemetered hourly averaged surface data via Iridium satellite, with Flex also transmitting hourly data from the subsurface instruments. High-resolution data are logged internally throughout the deployment in subsurface instruments, and downloaded upon recovery of the mooring. KE016 was the fifth KEO mooring to have phased out the ATLAS system and implemented the newer TFlex.

Position information associated with real-time data comes through the Iridium satellite network. Buoy latitude and longitude are transmitted to shore via three GPS devices on the Flex, TFlex, and $CO_2$ systems. The Flex GPS measurements are hourly and TFlex GPS measurements occur every six hours. Occasional position errors were spotted and removed during quality control operations.

The KEO mooring site is nominally at 32.3°N, 144.6°E. The actual anchor position is different for each deployment, and the slack line mooring has a watch circle radius greater than 5km. For users performing intercomparisons, it may be important to use the actual position of the buoy from the GPS data. Also, depths of the subsurface measurements will change over time on the slack mooring. Depths shown in the delivered KEO files represent the nominal location of the sensor on the mooring line. To determine the true depth of the measurement, use the accompanying pressure time series data.

## 2.1 Sampling Specifications

The following tables describe the high-resolution sampling schemes for the KE016 mooring, for both the primary and secondary systems. Observation times in data files are assigned to the center of the averaging interval. The Flex system sensors are usually considered primary, and the reasoning behind any substitutions are described in the relevant sections that follow.

**PRIMARY SENSORS**

| Measurement | Sample Rate | Sample Period | Sample Times | Recorded Resolution | Acquisition System |
|---|---|---|---|---|---|
| Wind Speed/Direction | 2 Hz | 2 min | 2359-0001, 0009-0011… | 10 min | FLEX |
| Air Temperature + Relative Humidity | 1 Hz | 2 min | 2359-0001, 0009-0011… | 10 min | TFLEX |
| Barometric Pressure | 1 Hz | 2 min | 2359-0001, 0009-0011… | 10 min | TFLEX |
| Rain Rate | 1 Hz | 1 min | 0000-0001, 0001-0002… | 1 min | TFLEX |
| Shortwave Radiation | 1 Hz | 1 min | 0000-0001, 0001-0002… | 1 min | TFLEX |
| Longwave Radiation (Thermopile, Case & Dome Temperatures) | 1 Hz | 1 min | 0000-0001, 0001-0002… | 1 min | TFLEX |
| Seawater Temperature, Pressure & Conductivity | 1 per 10 min | Instant. | 0000, 0010,… | 10 min | Internal |
| Ocean Currents (Point) | 1 Hz | 2 min | 2359-0001, 0009-0011… | 10 min | Internal |
| Ocean Currents (Profile) *Not deployed KE016* | N/A | N/A | N/A | N/A | N/A |
| GPS Position | 1 per hr | Instant. | 0000, 0100, … | 1 hr | FLEX |

**Table 2: Sampling parameters of the primary sensors on KE016.**

**SECONDARY SENSORS**

| Measurement | Sample Rate | Sample Period | Sample Times | Recorded Resolution | Acquisition System |
|---|---|---|---|---|---|
| Wind Speed/Direction | 2 Hz | 2 min | 2359-0001, 0009-0011… | 10 min | TFLEX |
| Air Temperature + Relative Humidity | 1 Hz | 2 min | 2359-0001, 0009-0011… | 10 min | FLEX |
| Barometric Pressure | 1 Hz | 2 min | 2359-0001, 0009-0011… | 10 min | FLEX |
| Rain Rate | 1 Hz | 1 min | 0000-0001, 0001-0002… | 1 min | FLEX |
| Shortwave Radiation | 1 Hz | 1 min | 0000-0001, 0001-0002… | 1 min | FLEX |
| Longwave Radiation (Thermopile, Case & Dome Temperatures) | 1 Hz | 1 min | 0000-0001, 0001-0002… | 1 min | FLEX |
| SSTC | 1 per 10 min | Instant. | 0000, 0010,… | 10 min | Internal |
| GPS Position | 1 per 6 hrs | Instant. | 0000, 0600, … | 6 hr | TFLEX |

**Table 3: Sampling parameters for the secondary sensors on KE016.**

## 2.2 Data Returns

Data returns are calculated from the highest-resolution data, comparing the number of records available to the total amount of records expected for the period. The following list shows the data returns from the surface and subsurface measurements from both acquisition systems.

KE016 data returns were affected by rapidly depleting Flex system batteries. Since the TFlex failed to report positions on this deployment, the Flex system was the only reliable GPS system on the buoy, as the $CO_2$ system reports less frequently, and often less reliably. In order to preserve battery, all Flex sensors were turned off on March 6, 2019 except for GPS, wind (an instrument with low power requirements), and subsurface telemetry. This choice balanced the needs of maximizing subsurface data returns with retaining the ability to locate the buoy. By distributing many TFlex surface sensors as primary, the deactivated Flex sensors had little effect on primary data return statistics, showing the value of redundancy in surface measurements. The Flex batteries lasted until recovery, with a final voltage of 8.9V, near its lower threshold.

**Flex 0006:**

```
Data Return Summary
2018-07-03 07:31:00 to 2019-09-26 05:25:00

Sensor      Deployed       Obs    Return
========================================
AT1            64787     35439     54.7% ** Turned off 3/6/19
AT2            64787     35439     54.7% **
RH1            64787     35439     54.7% **
RH2            64787     35439     54.7% **
WIND1          64787     64623     99.7%
BP1            64787     35439     54.7% **
RAIN1         647874    352208     54.4% **
SWR1          647874    352511     54.4% **
LWR1          647874    352559     54.4% **

Subsurface Temperature Profile
     1m        64787     64787    100.0%
     5m        64787     64787    100.0%
    10m        64787     36347     56.1%
    15m        64787         0      0.0% * Realtime data available
    20m        64787     64787    100.0%
    25m        64787     64787    100.0%
    35m        64787     60776     93.8%
    40m        64787     64787    100.0%
    50m        64787     20329     31.4%
    75m        64787     56583     87.3%
   100m        64787     61421     94.8%
   125m        64787     63774     98.4%
   150m        64787     64784    100.0%
   175m        64787     64787    100.0%
   225m        64787     64787    100.0%
```

| | | | | |
|---|---|---|---|---|
| 275m | 64787 | 64787 | 100.0% | |
| 325m | 64787 | 64787 | 100.0% | |
| 375m | 64787 | 64787 | 100.0% | |
| 425m | 64787 | 64787 | 100.0% | |
| 475m | 64787 | 64787 | 100.0% | |
| 525m | 64787 | 64787 | 100.0% | |
| 5617m | 64787 | 64787 | 100.0% | |
| 5651m | 64787 | 64787 | 100.0% | |
| 5652m | 64787 | 64787 | 100.0% | |

Subsurface Pressure Profile

| | | | | |
|---|---|---|---|---|
| 20m | 64787 | 64787 | 100.0% | |
| 25m | 64787 | 64787 | 100.0% | |
| 35m | 64787 | 60776 | 93.8% | |
| 40m | 64787 | 64787 | 100.0% | |
| 50m | 64787 | 20329 | 31.4% | |
| 75m | 64787 | 56583 | 87.3% | |
| 100m | 64787 | 61421 | 94.8% | |
| 125m | 64787 | 63774 | 98.4% | |
| 150m | 64787 | 64784 | 100.0% | |
| 175m | 64787 | 64787 | 100.0% | |
| 225m | 64787 | 64787 | 100.0% | |
| 275m | 64787 | 64787 | 100.0% | |
| 325m | 64787 | 64787 | 100.0% | |
| 375m | 64787 | 64787 | 100.0% | |
| 425m | 64787 | 64787 | 100.0% | |
| 475m | 64787 | 64787 | 100.0% | |
| 525m | 64787 | 64787 | 100.0% | |
| 5617m | 64787 | 64787 | 100.0% | |
| 5651m | 64787 | 64787 | 100.0% | |
| 5652m | 64787 | 64787 | 100.0% | |

Subsurface Salinity Profile

| | | | | |
|---|---|---|---|---|
| 1m | 64787 | 64787 | 100.0% | |
| 10m | 64787 | 30626 | 47.3% | |
| 15m | 64787 | 0 | 0.0% | * Realtime data available |
| 25m | 64787 | 64787 | 100.0% | |
| 35m | 64787 | 60776 | 93.8% | |
| 50m | 64787 | 20329 | 31.4% | |
| 75m | 64787 | 56583 | 87.3% | |
| 100m | 64787 | 61421 | 94.8% | |
| 125m | 64787 | 63774 | 98.4% | |
| 150m | 64787 | 64784 | 100.0% | |
| 175m | 64787 | 64787 | 100.0% | |
| 225m | 64787 | 64787 | 100.0% | |
| 275m | 64787 | 64787 | 100.0% | |
| 325m | 64787 | 64787 | 100.0% | |
| 425m | 64787 | 64787 | 100.0% | |
| 525m | 64787 | 64787 | 100.0% | |
| 5617m | 64787 | 64787 | 100.0% | |
| 5651m | 64787 | 64787 | 100.0% | |
| 5652m | 64787 | 64787 | 100.0% | |

AQD Current Velocity

| | | | | |
|---|---|---|---|---|
| 8m | 64787 | 24729 | 38.2% | |
| 16m | 64787 | 0 | 0.0% | * Realtime data available |
| 36m | 64787 | 53338 | 82.3% | |

**TFlex 2004:**

Data Return Summary
2018-07-03 07:31:00 to 2019-09-26 05:25:00

| Sensor | Deployed | Obs | Return |
|---|---|---|---|
| AT1 | 64787 | 64697 | 99.9% |
| RH1 | 64787 | 64697 | 99.9% |
| WIND1 | 64787 | 43711 | 67.5% |
| BP1 | 64787 | 64697 | 99.9% |
| RAIN1 | 647874 | 643124 | 99.3% |
| SWR1 | 647874 | 618377 | 95.4% |
| LWR1 | 647874 | 559725 | 86.4% |
| SST1 | 64787 | 52170 | 80.5% |
| SSC1 | 64787 | 52170 | 80.5% |
| SSS1 | 64787 | 52170 | 80.5% |

## 2.3 Known Sensor Issues

The primary sensor issues on KE016 stemmed from physical damage to individual instruments which cascaded down the line, early battery depletion, and the Flex system's above-average battery drain.

Two separate instrument cascades occurred, each involving 3 instruments. In the first, the 8m AQD (S/N 12026) and 10m SBE37 (S/N 7793) came to rest on the 15m SBE37 (S/N 9412), which was found flooded, but the 15m batteries looked freshly shorted and were warm, indicating that the flooding may have occurred during the routine movements associated with recovery. The only pressure sensor in this pileup was housed within the 8m aquadopp, whose data ended on 12/22/2018. At that time, the aquadopp was near its proper, nominal depth, so the time of the slide was indeterminate. The 10m instrument began recording irregular timestamps and corrupt data lines to memory on 3/12/2019, characteristic of battery failure. The record is truncated to this date, since the data thereafter couldn't be corrected with confidence, and differences between the 10m and 15m data records suggests the cascade occurred after the 10m instrument's battery failure. The 15m instrument flooded, so only its realtime data exist and are distributed.

The second cascade occurred with the 16m AQD (S/N 6290) and the 20m SBE39 (S/N 4861), which came to rest on the 25m SBE37 (S/N 7103). The 16m AQD batteries failed before the cascade, and no data were recovered from that instrument, but the 20m pressure data indicate the 20m sensor came to rest at 25m gradually throughout the day on 9/14/2019, after which the 20m data were flagged Q4 (lower quality). The 20m and 40m instruments were deployed inverted in accordance with the mooring diagram, but according to the recovery logs, the SBE37 at 50m (S/N 7105) was also inverted.

Two Aquadopp current meters (S/N 6290 at 16m and S/N 6808 at 36m) did not download in the field, but S/N 6808 later downloaded at the lab, after fixing some damaged internal wires. No repair was possible on S/N 6290, which had short-circuited, charring internal wires and damaging the electronics. Realtime data remains available from this instrument, but no download attempts were successful.

The 425m instrument (S/N 7780) was the final sensor noticeably displaced from its nominal position. It slid to 475m and was recovered with heavy damage and a missing shield, but pressure data indicate it remained in place during the deployment. Combined with the 15m sensor's warm batteries which likely indicated a failure/flooding during recovery, it is speculated that this recovery produced more strain or vibration in the nilspin line than past operations. Despite a damaged inductive modem and cracked pressure housing on the 425m instrument, data were downloaded successfully.

Low batteries were noted on several subsurface instruments and verified by cross-referencing each instrument's status upon recovery with the timing of realtime data dropouts. All battery failures are listed below, along with the serial number, instrument depth, and the time of each instrument's final recorded timestamp.

| Serial Number (Depth) | Final Timestamp (UTC) | Comment |
|---|---|---|
| 12026 (8m) | 12/22/2018 1:00 | Aquadopp Current Meter |
| 7793 (10m) | 3/12/2019 18:10 | Irregularly sampled timestamps thereafter |
| 9412 (15m) | 8/29/2019 3:00 | Dead Battery / Flooded (only Realtime data) |
| 6290 (16m) | 3/31/2019 16:00 | Aquadopp short circuited (only Realtime data) |
| 7104 (35m) | 8/30/2019 16:30 | Low Battery |
| 6808 (36m) | 7/10/2019 10:30 | Aquadopp Current Meter |
| 7105 (50m) | 11/21/2018 15:00 | Low Battery |
| 7106 (75m) | 7/31/2019 9:00 | Low Battery |
| 7107 (100m) | 9/2/2019 22:00 | Low Battery |
| 7108 (125m) | 9/19/2019 6:50 | Low Battery |

**Table 4: Battery failures on KE016 instrumentation.**

The final substantial data issue was caused by the above-average power draw from the Flex acquisition system, which was mitigated by shutting off most Flex surface sensors on March 6, 2019. This action preserved power to extend the system's lifetime, which served to keep subsurface realtime data flowing, while also retaining the ability to locate the buoy during recovery. To distribute the most complete records, the TFlex surface sensors, with the exception of winds, were designated primary.

Acquisition system resets were a minor issue on KE016 for both the Flex and TFlex systems, which began independently resetting at weekly intervals in March and January of 2019, respectively. This weekly reset pattern is largely benign, but could contribute to a minor increase in power consumption and interference if a reset coincides with sampling. Since the only system configuration set for 1 week (168 hours) is the radio frequency (RF) period, during which commands can be sent to the buoy from a nearby vessel, the leading hypothesis is an error in this particular system's RF programming.

Three deep SBE instruments were deployed on KE016 in an attempt to learn more about persistent salinity drift observed by unpumped Seabird instruments. Two unpumped instruments (S/N 11926 and S/N 12243) displayed the false yearlong freshening trend characteristic of KEO's near-bottom deployments, which is attributed to sediment infiltrating the conductivity cell. Seabird Inc. loaned OCS a pumped instrument (S/N 11456), hoping the pump would resolve the issue of near-bottom salinity drift. Unfortunately, the pumped instrument's data were unrealistic: high values >35 PSU abruptly dropped to ~27 PSU in the first month of the deployment, rendering it unusable. Deep ocean climatology at KEO, combined with the two unpumped instruments, suggests that abyssal salinity remains near 34.69 PSU.

# 3.0 Data Processing

Processing of data from OCS moorings is performed after the data are returned to PMEL. There are some differences between OCS data and data from GTMBA moorings, but standard methods described below are applied whenever possible. The process includes assignment of quality flags for each observation, which are described in Appendix A. Any issues or deviations from standard methods are noted in processing logs and in this report.

Raw data recovered from the internal memory of the data acquisition system are first processed using computer programs. Instrumentation recovered in working condition is returned to PMEL for post-recovery calibration before being reused on future deployments. These post-recovery calibration coefficients are compared to the pre-deployment coefficients. If the comparison indicates a drift larger than the expected instrument accuracy, the quality flag is lowered for the measurement. If post-recovery calibrations indicate that sensor drift was within expected limits, the quality flag is raised. Post-recovery calibrations are not generally applied to the data, except for seawater salinity, or as otherwise noted in this report. Failed post-recovery calibrations are noted, along with mode of failure, and quality flags are left unchanged to indicate that pre-deployment calibrations were applied and sensor drift was not estimated.

The automated programs also search for missing data, and perform gross error checks for data that fall outside physically realistic ranges. A computer log of potential data problems is automatically generated as a result of these procedures.

Time series plots, difference plots, and comparison plots are generated for all data. Plots of differences between adjacent subsurface temperature measurements are also generated. Statistics, including the mean, median, standard deviation, variance, minimum and maximum are calculated for each time series.

Trained analysts examine individual time series and statistical summaries. Data that have passed gross error checks, but which are unusual relative to neighboring data in the time series, or which are statistical outliers, are examined on a case-by-case basis. Mooring deployment and recovery logs are searched for corroborating information such as battery failures, vandalism, damaged sensors, or incorrect clocks. Consistency with other variables is also checked. Data points that are ultimately judged to be erroneous are flagged, and in some cases, values are replaced with “out of range” markers. For a full description of quality flags, refer to Appendix A.

For some variables, additional post-processing after recovery is required to ensure maximum quality. These variable-specific procedures are described below.

## 3.1 Buoy Positions

Since KEO is a slack-line mooring with a long scope, the buoy has a watch circle radius of more than 5km. When using KEO data in scientific analyses, it may be appropriate to consider the actual GPS position of the buoy rather than its nominal position. Gross error checking was performed to eliminate values outside the watch circle, but no further processing was performed, and positions inside the watch circle were used to determine buoy velocities for processing ocean current data.

## 3.2 Meteorological Data

All primary meteorological sensors on KE016 remained functional at or near 100% throughout the deployment. Many TFlex instruments were considered primary in this deployment due to higher data returns and the Flex power issue.

No data from secondary sensors are included in the final data files, except when included in OceanSITES files as secondary data. The OceanSITES data repository can be found here: http://dods.ndbc.noaa.gov/thredds/catalog/oceansites/DATA/KEO/catalog.html

The KE016 buoy had secondary air temperature, relative humidity, wind, rain, air pressure, and radiation sensors. The only tertiary sensor deployed was a Rotronic HygroClip attached to the Flex system, measuring air temperature and relative humidity. These tertiary data were not distributed in any format.

### 3.2.1 Winds

Wind sensors performed well on KE016, with the exception of the TFlex record, which became intermittent in May 2019 and reported increasingly sparse data after mid-May in 2019. Thus, the Flex winds are distributed as the primary wind data, and extend throughout the deployment.

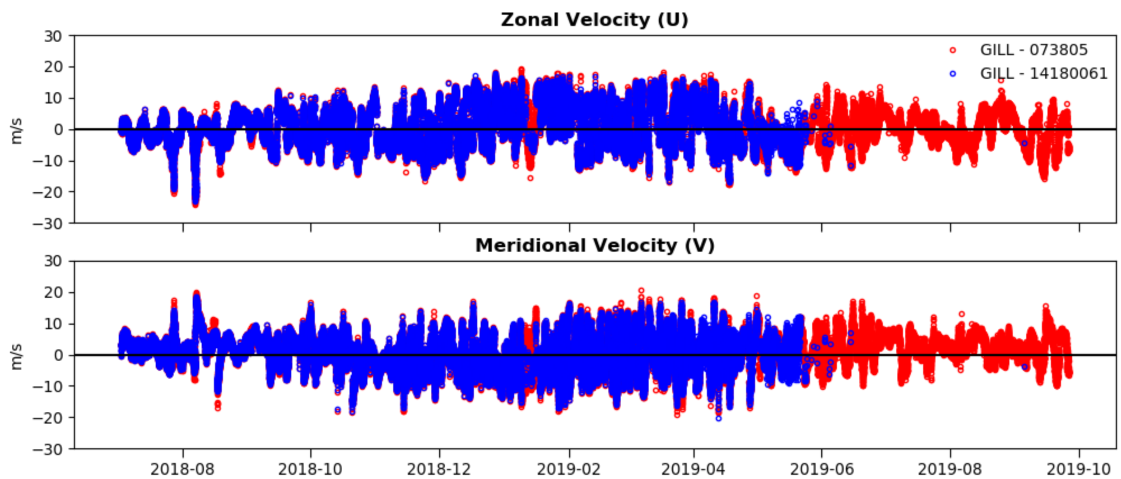


Figure 5: Eastward and northward winds on KE016.

Both wind sensors sustained some damage during recovery, with the TFlex wind sensor dangling from its cable after the mast impacted the ship's hull. However, both sensors survived and passed their post-calibration procedures, with maximum residuals of the least-squares fit (compared against a gold standard) of -0.09 m/s (Flex) and -0.16 m/s (TFlex). Mean errors across all speeds in the wind tunnel were low (<0.1 m/s). Default quality flags (Q2) were assigned and gross error thresholds were applied to the wind records, but no adjustments or additional processing was required.

### 3.2.2 Air Temperature

Air temperature sensors performed well, passing all pre- and post-calibration procedures. The TFlex data were primary due to a more complete record, after the Flex sensor was powered off to save system batteries. No other issues were noted with the air temperature records, and differences between the Flex and TFlex MP101s were centered around zero, indicating the sensors didn't drift while jointly active.

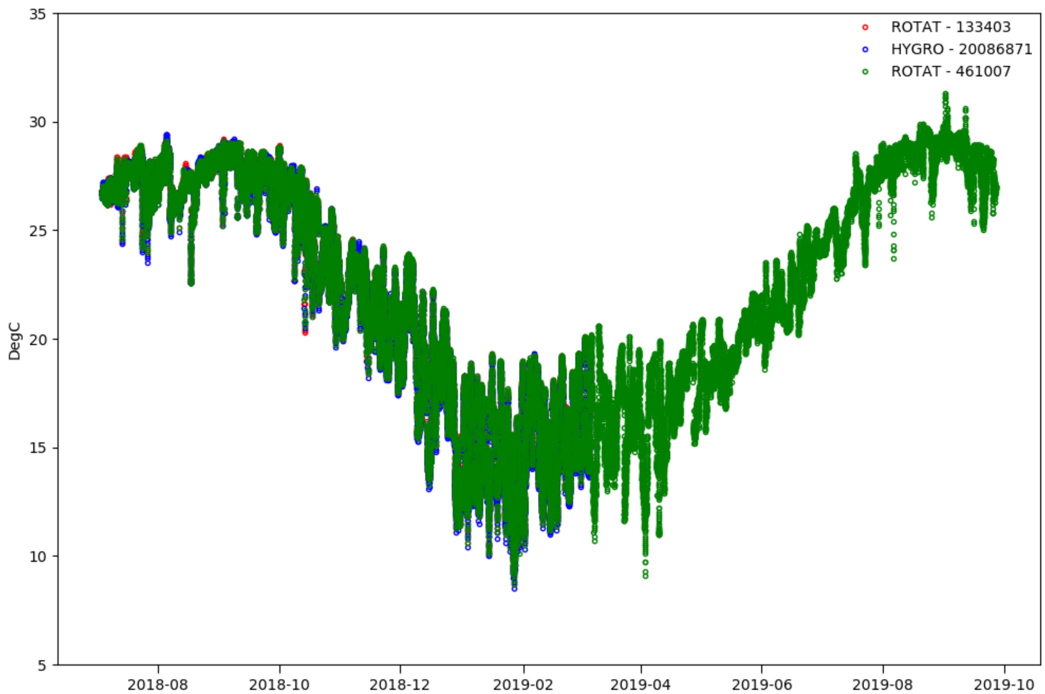


**Figure 6: Air temperature on KE016.**

### 3.2.3 Relative Humidity

The TFlex relative humidity sensor was distributed as primary because its records were more complete after the Flex sensor was powered off. However, the TFlex RH failed its post-calibration. Failed post-calibrations warrant increased scrutiny of the underlying data, and often a quality downgrade when paired with drift, gross outliers, or other signs of failure. After review, the decision was made to assign standard Q2 flags to the data because 1) the lack of corroborating indicators of failure and 2) the TFlex humidity data were within sensor specification thresholds when examined against the subsequent deployment's 3x freshly-calibrated ATRH sensors, making for a continuous handoff between deployments (not shown).

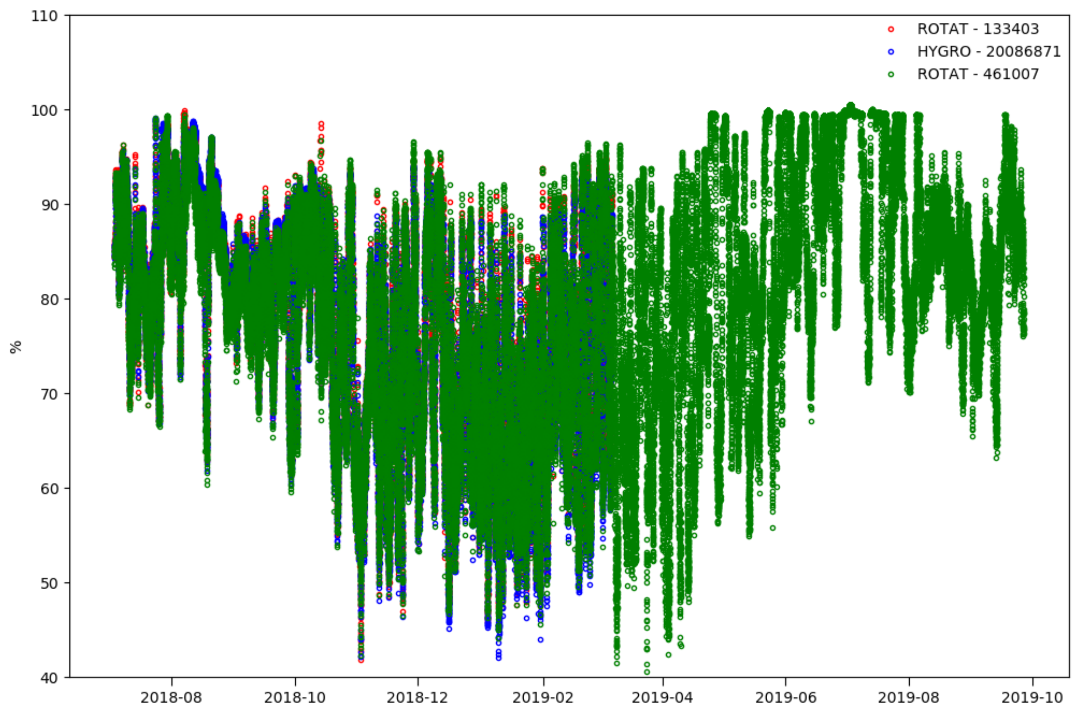


**Figure 7: Relative humidity on KE016.**

### 3.2.4 Barometric Pressure

The redundant Druck barometers both functioned effectively within the context of the partial Flex shutdown. Calibrations were applied in post-processing, as the Druck barometers are well-documented as not applying the calibrations loaded into the Flex/TFlex systems in the field. Standard quality flags (Q2) were assigned to the final, calibrated data.

The Druck barometers are slated to be phased out in future deployments, with the GE8100 TERPS sensors providing a more stable and higher-quality measurement at a similar cost. Initial results have shown the new sensor more consistently matches the gold standard (Paros) sensor during testing at PMEL.

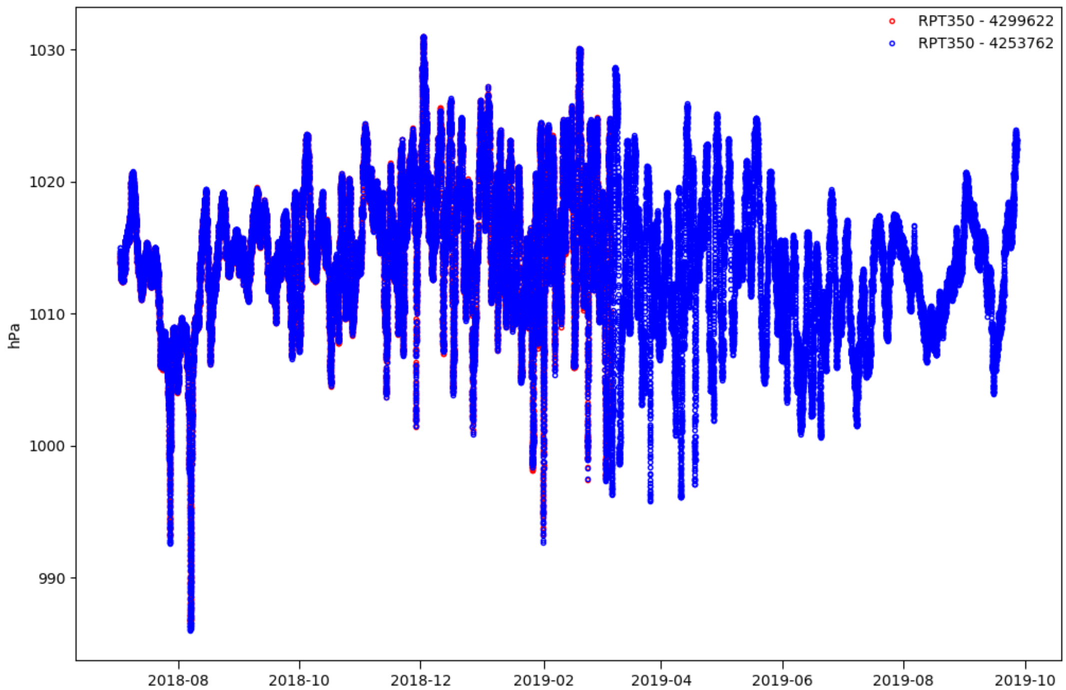


**Figure 8: Barometric pressure on KE016.**

### 3.2.5 Rain

Rain data are acquired as accumulation values, and then converted to rain rates during processing. Rainfall data are collected using an RM Young rain gauge, and recorded internally at a 1-min sample rate. The gauge consists of a 500mL catchment cylinder which, when full, empties automatically via a siphon tube. Data from a three minute period centered near siphon events are ignored. Occasional random spikes in the accumulation data, which typically occur during periods of rapid rain accumulation, or immediately preceding or following siphon events, are eliminated manually.

To reduce instrumental noise, internally recorded 1-minute rain accumulation values are smoothed with a 16-minute Hanning filter upon recovery. These smoothed data are then differenced at 10-minute intervals and converted to rain rates in mm/hr. The resultant rain rate values are centered at times coincident with other 10-minute data (0000, 0010, 0020...).

Residual noise in the filtered data may include occasional false negative rain rates, but these rarely exceed a few mm/hr. No wind correction is applied, as this is expected to be done by the user. The wind effect can be large. According to the Serra, et al. (2001) correction scheme, at wind speeds of 5 m/s the rain rates should be multiplied by a factor of 1.09, while at wind speeds of 10 m/s, the factor is 1.3. As winds are high at KEO, the user is strongly encouraged to apply an appropriate wind correction.

The post-mission TFlex rain sensor passed a bench check, but a new sensor tube was installed for future use. The old sensor tube, which had been out on the KE016 deployment, was noted as being unstable and full of debris, but passed calibrations, so no changes were made to the rain data quality outside of the routine quality control steps.

### 3.2.6 Shortwave Radiation

The primary shortwave radiation sensor was chosen based on a system developed by Kelly Balmes during the summer of 2014, using the following criteria:

- Use the sensor with the higher shortwave daily average (if difference is > 1%)
- Use the FLEX system if all else is similar
- Use the sensor that maximizes the time period of available data

Based on these criteria, the KE016 TFlex shortwave radiometer was designated primary. The TFlex sensor had substantially higher data returns, and mean daily Flex and TFlex shortwave radiation values were compared and found to differ by 0.4%, leading to the choice of sensor that maximizes available data.

Shortwave radiation is processed into hourly and daily averaged values differently than other measurements. Because SWR goes to 0 at night, any substantial number of missing values during the night (day) will bias the data high (low). In keeping with GTMBA processing, the percentage of good high-resolution data for SWR must be at least 87.5% in order to generate an hourly or daily averaged data point. Most other instruments use a 50% threshold for high-resolution data needed to generate hourly and daily averages.

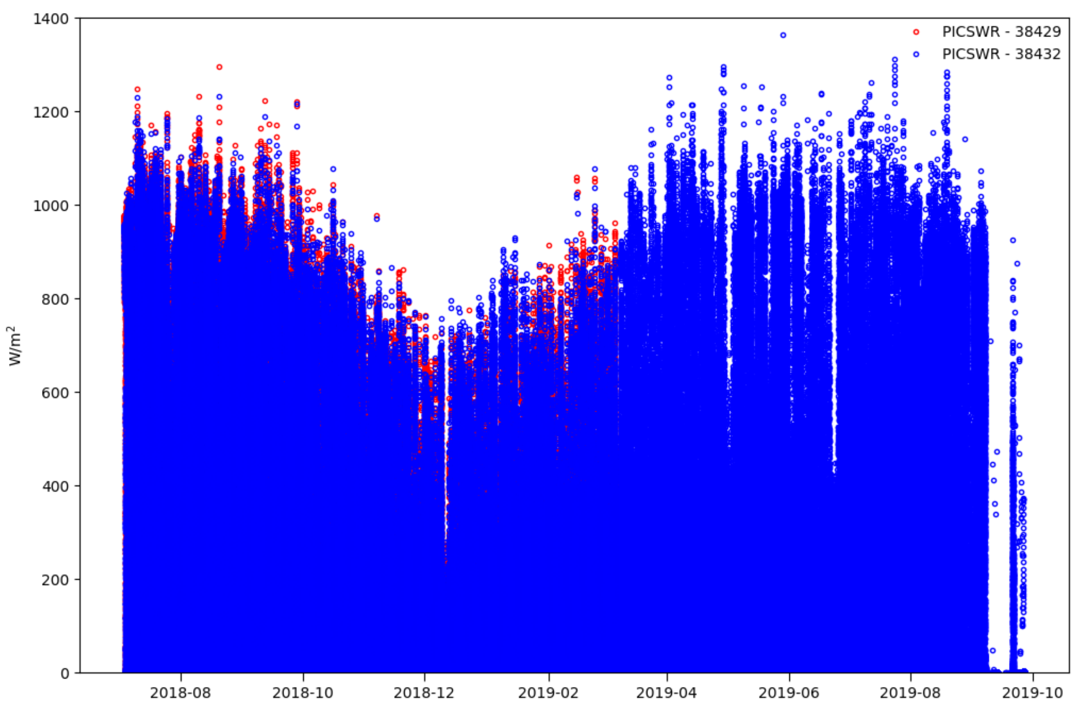


**Figure 9: Raw shortwave radiation data from KE016.**

### 3.2.7 Longwave Radiation

The downwelling longwave radiation is computed from thermopile voltage, dome temperature, and instrument case temperature measurements, using the method described by Fairall et al. (1998).

Kelly Balmes also developed a set of criteria for determining the primary LWR sensor:

- Use the LWR data from the sensor on the data system that was chosen for SWR
- If LWR data from the first criteria is not available, use the remaining instrument

These criteria were created to maximize data returns and account for bent radiation masts, which are usually detectable by comparing SWR measurements. Although LWR is much less sensitive to orientation, a bent mast can affect either sensor. Clear sky conditions will have a lower LWR than clouds, which are warm due to water content (high LWR). With one LWR and one SWR sensor mounted to each mast, the goal of the criteria is to obtain data from the most vertical mast to avoid a mean tilt when samples are averaged over 1 minute. Based on these criteria, the KE016 TFlex LWR was primary.

Regions of unrealistically high, noisy LWR data which exceeded climatological norms were again seen on this deployment during the hottest part of the year (see the spiky anomaly in the raw, high-resolution data of Figure 10, and the cleaned-up LWR data in Appendix B1). This issue has been observed before, but no discernable pattern links it to a particular instrument or acquisition system. The instrument manufacturer (Eppley) suggested that bad thermopile readings are the underlying cause of these anomalous spikes. In the absence of an inversion, net LWR should not exceed 0 W/m$^2$, which would indicate heat transfer from the atmosphere to the ocean.

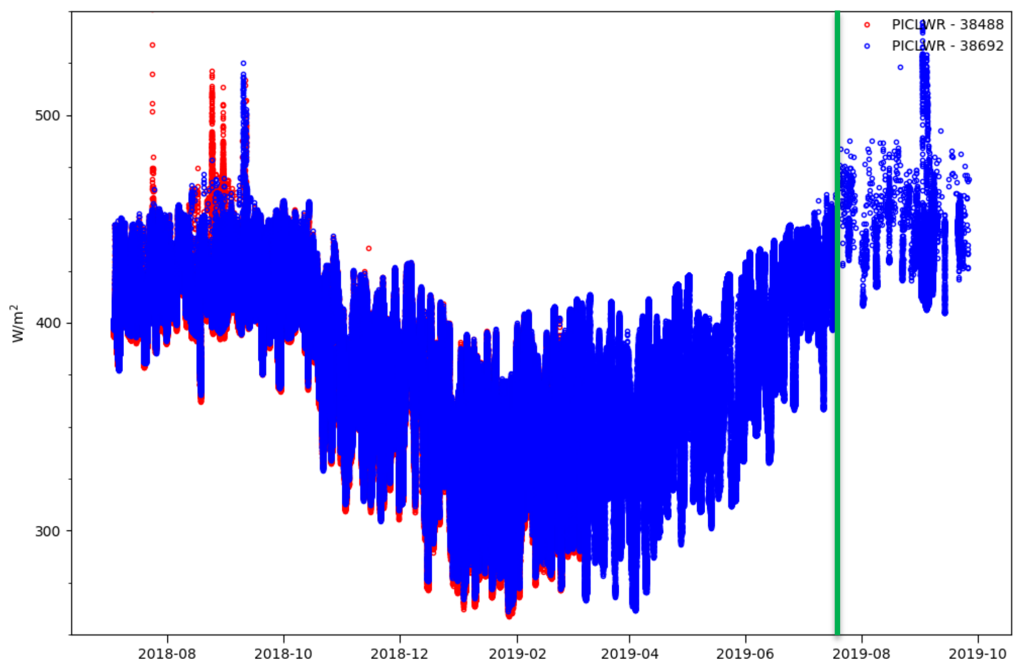


**Figure 10: Raw downwelling longwave radiation data on KE016. The green line indicates an apparent regime shift in sampling, which warranted a quality downgrade in the subsequent data.**

Backing up Eppley's hypothesis, SST exceeded air temperature at the time of the anomalies, indicating sensible heat transfer from ocean to atmosphere. Unless other heat transfers (e.g. latent heat) are downward and of greater magnitude, this observation is inconsistent with a positive net LWR. Additionally, the Stefan Boltzman equation suggests a downwelling LWR limit of ~478.9 W/m$^2$, given the observed maximum air temperature of ~30°C. However, these do not necessarily prove that net LWR is incorrect, because LWR is a product of the entire overlying atmosphere.

If Eppley's hypothesis is correct, the explanation could reside in the gain that is applied to the thermopile voltage before being interpreted by the acquisition system. Q5 flags (removed) were applied to downwelling LWR when net LWR was greater than 0 or where downwelling exceeded the expected seasonal norms (thresholded at 475 W/m$^2$), and seasonal outliers were removed manually. LWR data were otherwise distributed with standard quality flags, with the one exception being Q4 flags applied to the TFlex LWR after 7/18/2019, when 1) the sensor sampling changed, 2) the system began recording a moderate number of missing data points, often leaving the remaining data points without context and 3) there appears to be a slight upward-shift or regime change in the measurements after this time. Both LWR sensors passed calibrations, but the Q4 data remain suspect.

## 3.3 Subsurface Data

OCS KEO moorings are instrumented from the surface down to 525m, with one or more deep T/S instruments attached to the acoustic release or other locations near the seafloor. Redundant sea surface temperature and conductivity (SSTC) instruments are deployed on the bridle, which are wired to the Flex and TFlex systems, respectively.

All remaining subsurface instrumentation was connected inductively to the Flex system, except for the deep instruments attached to the acoustic release. Clock errors from each recovered subsurface instrument are summarized in Table 5. Since no clock errors exceeded half the sampling interval, measurements were mapped to the nearest 10-minute time increment.

The instrument at 15m (S/N 9412) did not report a clock error because it had flooded, so no interaction with this instrument was possible and only realtime data exist at that depth.

| Type | Serial | Real Time | Inst Time | Clock Error |
|---|---|---|---|---|
| SBE37-TC-SMP | 12520 | 11:11:11 | 11:10:56 | -0:00:15 |
| SBE37-TC-SMP | 11552 | 11:03:05 | 11:03:04 | -0:00:01 |
| SBE39-T-IM | 3283 | 23:36:20 | 23:36:57 | 0:00:37 |
| SBE37-TC | 7793 | 9:48:00 | 9:48:31 | 0:00:31 |
| SBE37-TC | 9412 | | | |
| SBE39-TP-IM | 4861 | 23:06:25 | 23:07:39 | 0:01:14 |
| SBE37-TCP | 7103 | 9:11:11 | 9:11:38 | 0:00:27 |
| SBE37-TCP | 7104 | 9:57:00 | 9:57:24 | 0:00:24 |
| SBE39-TP-IM | 4857 | 23:29:00 | 23:30:11 | 0:01:11 |
| SBE37-TCP | 7105 | 9:39:35 | 9:39:55 | 0:00:20 |
| SBE37-TCP | 7106 | 8:53:35 | 8:54:11 | 0:00:36 |
| SBE37-TCP | 7107 | 6:49:20 | 6:49:36 | 0:00:16 |
| SBE37-TCP | 7108 | 6:39:40 | 6:40:25 | 0:00:45 |
| SBE37-TCP | 9413 | 6:22:30 | 6:22:37 | 0:00:07 |
| SBE37-TCP | 7781 | 7:01:45 | 7:02:12 | 0:00:27 |
| SBE37-TCP | 7782 | 7:11:00 | 7:11:32 | 0:00:32 |
| SBE37-TCP | 7783 | 9:02:45 | 9:03:11 | 0:00:26 |
| SBE37-TCP | 7784 | 7:21:40 | 7:21:59 | 0:00:19 |
| SBE39-TP-IM | 4360 | 23:41:30 | 23:42:33 | 0:01:03 |
| SBE37-TCP | 7780 | 9:19:25 | 9:20:08 | 0:00:43 |
| SBE39-TP-IM | 4378 | 23:21:10 | 23:22:35 | 0:01:25 |
| SBE37-TCP | 7092 | 7:31:20 | 7:31:56 | 0:00:36 |
| SBE37-TC-SMP | 12243 | 7:43:55 | 7:43:52 | -0:00:03 |
| SBE37-TC-SMP | 11926 | 10:38:10 | 10:38:17 | 0:00:07 |
| SBE37-TC-SMP | 11456 | 10:44:50 | 10:44:47 | -0:00:03 |

**Table 5: KE016 instrument clock errors.**

### 3.3.1 Temperature

Subsurface temperature instruments were set to 10-minute sampling increments. The data are also provided at hourly and daily resolutions. Temperatures are rarely corrected based on post-calibrations, and there was no evidence of drifting temperature measurements.

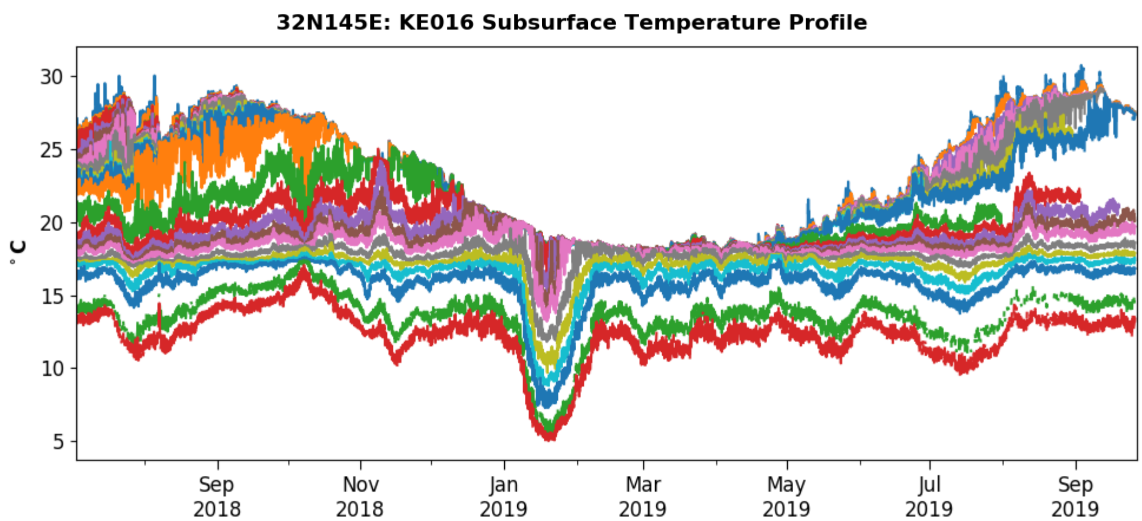


**Figure 11: Realtime KE016 subsurface temperature data (surface to 525m).**

A slow-moving cold-core eddy passed the KEO mooring in January 2019, as depicted in Figure 11. As the eddy approached and departed the station, all instruments were drawn upward in the water column. The effect was more prominent with depth, with the 525m instrument nearing 475m (see pressure data in Figure 12), and at the eddy's center, a 525m temperature anomaly approaching 10°C was observed.

### 3.3.2 Pressure

Since this was a slack mooring, none of the sensors can be assumed to have been recording measurements at their nominal depths. Users are reminded that the depths of subsurface sensors must be computed from the observed and interpolated pressures contained in the data files.

Pressure measurements were recorded by most of the subsurface instruments. In processing for salinity, interpolated pressures were used if an instrument's pressure sensor failed. In the case of complete instrument failure, where no temperature or conductivity data exists, interpolated pressures were truncated to the time of failure.

An unusual pressure signature was observed during the first month of the KE016 deployment, when the 525m instrument consistently reported pressures near 500 dbar. It is hypothesized that a twist in the nilspin during deployment caused the 525m instrument to catch on the passive acoustic listening device (PAL) at 500m. During typhoon Jongdari, pressure data showed the instrument returning to its nominal depth, presumably indicating the self-correction of any twist or knot. Data were flagged Q4 (lower quality) until the 525m instrument settled to its nominal position.

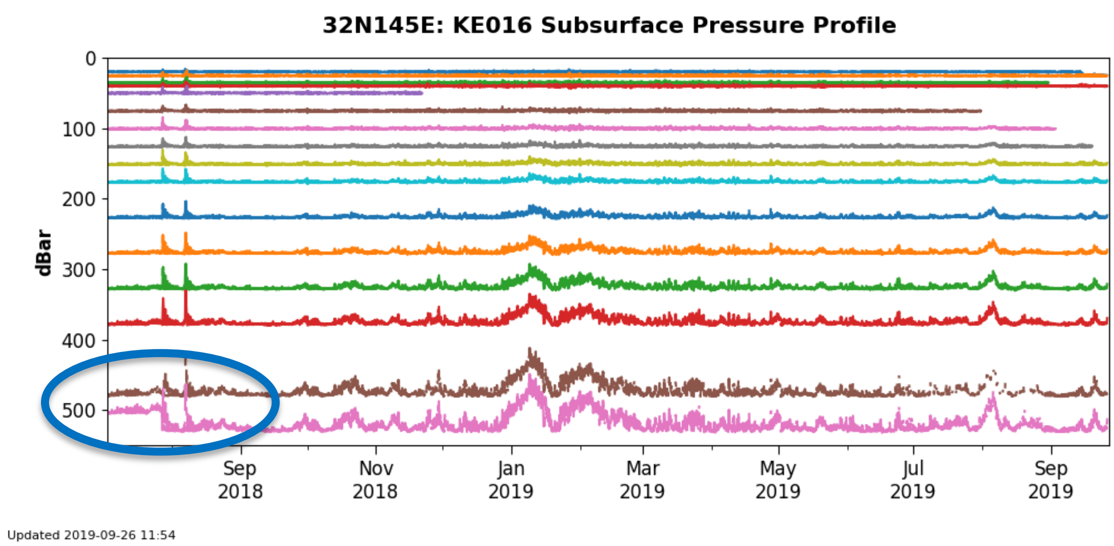


**Figure 12: Realtime KE016 subsurface pressure data. The 525m instrument (pink line) notably resided at ~500m (circled in blue) until coming to rest at its nominal depth after typhoon passage.**

### 3.3.3 Salinity

Salinity values were calculated from measured conductivity and temperature data using the method of Fofonoff and Millard (1983). Conductivity values from all depths were adjusted for sensor calibration drift by linearly interpolating over time between values calculated from the pre-deployment calibration coefficients and those derived from the post-deployment calibration coefficients. Salinities were calculated from both the pre and post conductivity values, to determine the drift in the salinity measurement.

Salinity Drifts in PSU (post - pre):

| **Depth:** | **Drift:** |
|---|---|
| 1m (TFlex) | -0.0576 |
| 1m (Flex) | -0.0281 |
| 10m | -0.0125 |
| 15m | N/A (only realtime data available; no post-calibration) |
| 25m | -0.0913 |
| 35m | -0.0467 |
| 50m | -0.0275 |
| 75m | -0.0558 |
| 100m | -0.0526 |
| 125m | -0.0484 |
| 150m | -0.0326 |
| 175m | -0.0676 |
| 225m | -0.0463 |
| 275m | -0.0469 |
| 325m | -0.0378 |
| 425m | -0.0952 |
| 525m | -0.0118 |

The values above indicate the change in data values when post-recovery calibrations are applied vs. when pre-deployment calibrations are applied. Negative differences suggest that the instrument drifted towards higher values while deployed, and indicate expansion of the conductivity cell effective cross-sectional area. This expansion is possibly due to scouring of the cell wall by abrasive material in the sea water. Positive values indicate decrease in the cell effective cross-sectional area, presumably due to fouling, and secondarily due to fouling or loss of material on the cell electrodes.

A thirteen-point Hanning filter was applied to the high-resolution (ten-minute interval) conductivity and temperature data. A filtered value was calculated at any point for which seven of the thirteen input points were available. The missing points were handled by dropping their weights from the calculation, rather than by adjusting the length of the filter. Salinity values were then recalculated from the filtered data.

## Manual Salinity Adjustments

The drift-corrected salinities were checked for continuity across deployments. The range and magnitude of variation matched well with prior and subsequent deployments.

Additional linear corrections were also applied to the salinity data in time segments, as noted below. These corrections were based on comparisons with neighboring sensors on the mooring line. If an unrealistic prolonged, unstable density inversion was found, an attempt was made to identify the sensor at fault and adjust its data based on differences with data from adjacent depths during unstratified conditions (e.g. within the mixed layer during nighttime). These *in situ* calibration procedures are described by Freitag et al. (1999).

Based on manual review of the data against neighboring instruments, the following adjustments were made:

2018-07-03 09:40:00 to 2019-09-26 05:20:00 at 35 m adjusted -0.0120 to -0.0120
2018-08-06 21:33:35 to 2019-09-26 05:20:00 at 25 m adjusted 0.0000 to 0.0200
2019-03-10 10:05:43 to 2019-04-25 09:25:14 at 1m TFlex adjusted 0.0000 to -0.0150
2019-04-25 09:25:14 to 2019-05-18 12:47:08 at 1m TFlex adjusted -0.0150 to -0.0110
2019-05-18 12:47:08 to 2019-07-01 08:16:37 at 1m TFlex adjusted -0.0110 to 0.0130

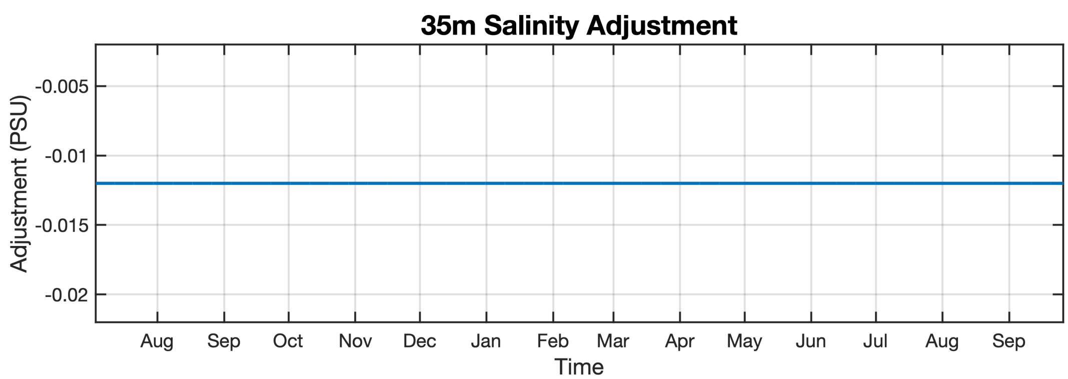


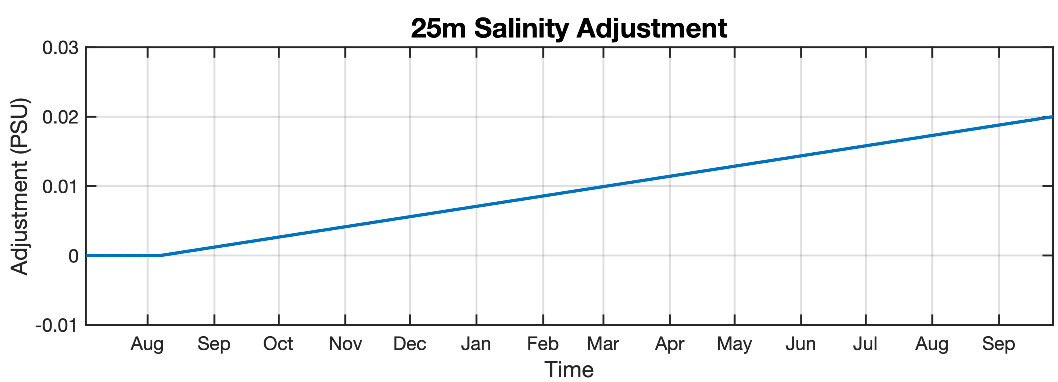

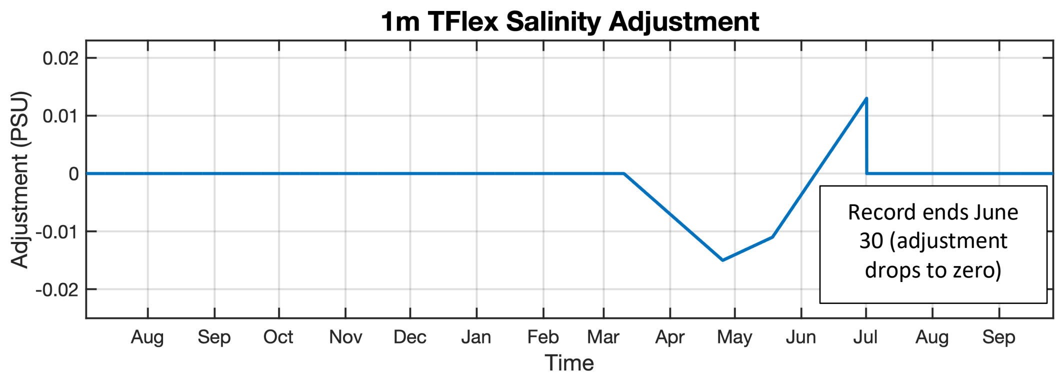


Comparisons against CTDs taken near the KE016 mooring did not warrant any further adjustments to the subsurface data.

### 3.3.4 Deep SBE Data

From PA006-present and KE010-present, an SBE37S has been mounted on the acoustic release near the anchor. Retrieval rates have been high, and several years of data at each site are now available.

Because deep SBE instruments at KEO have repeatedly drifted fresh 0.03 – 0.06 PSU each year at KEO before immediately recovering to climatological values during ascent from depth, additional deep instruments were deployed on KE016 to investigate the drift. A pumped SBE (S/N 11456) was deployed alongside the "primary" unpumped deep instrument (S/N 11926) at 56m above the seafloor, and an additional unpumped instrument (S/N 12243) was deployed about 90m off the seafloor. Early information about this drift can be found in OCS Technical Note 9, with a more complete description in Anderson et al. (2020).

Unfortunately, the pumped instrument, deployed in an attempt to circumvent the effects of the hypothesized sediment accumulation in the conductivity cell and resultant drift, failed to report usable salinity/conductivity/density. The data written to memory were well outside the expected climatological range of the abyssal ocean (>35 PSU, then immediately <28 PSU). The additional deployment of S/N 12243 at 90m off the seafloor was an attempt to escape the sediment-laden nepheloid layer altogether, but this instrument still experienced the false, freshening drift. The best available data was from the 56m unpumped instrument, which is distributed on the OCS DisDel page. Data from all 3 are distributed in OceanSITES format, with the exception of the conductivity, salinity, and density records from S/N 11456, which were hard flagged as being out-of-range (Q5).

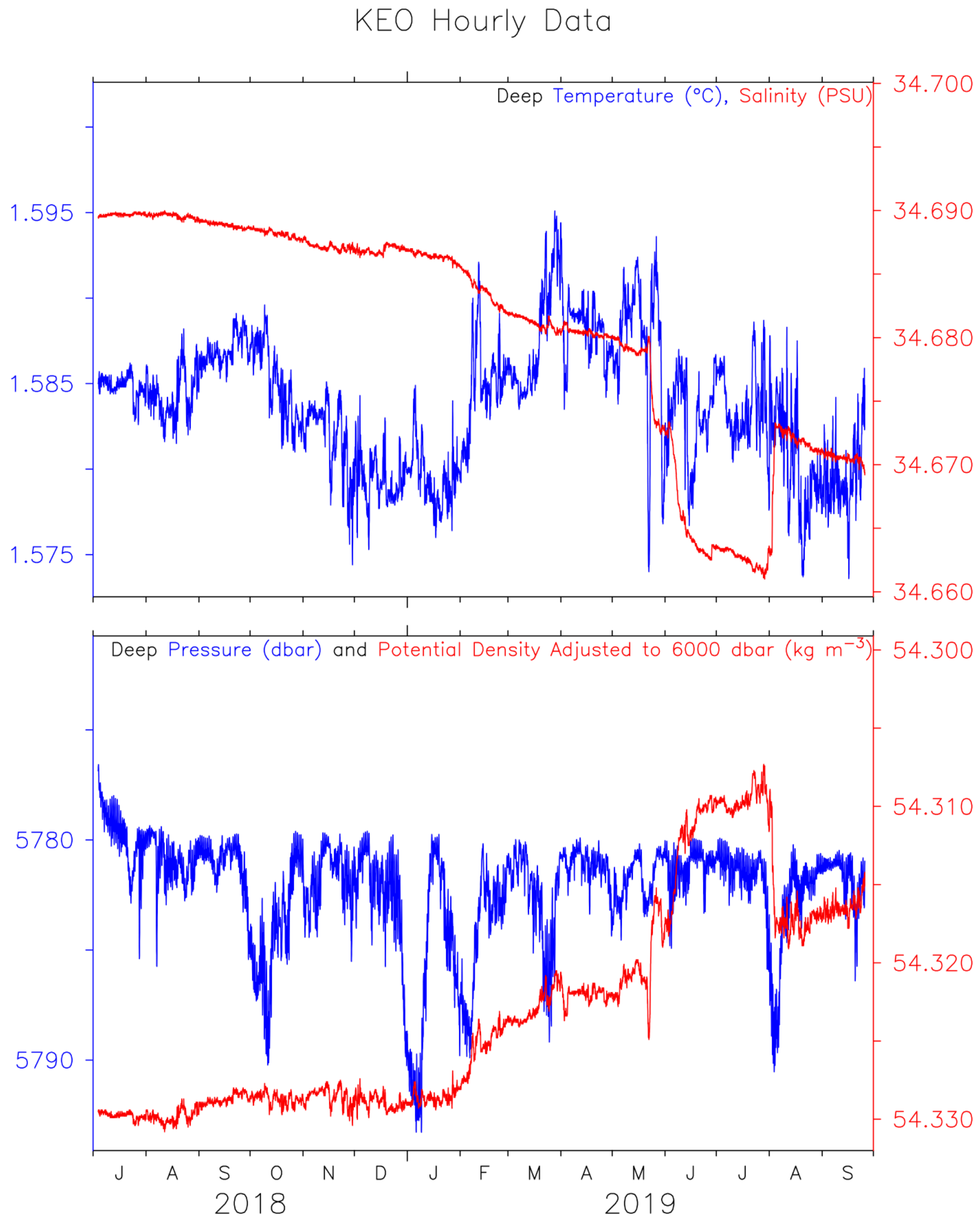


**Figure 13: Deep SBE temperature, pressure, salinity and potential density time-series calculated using pre-calibration coefficients.**

Deep SBE data at KEO are distributed with pre-calibration coefficients applied (see Figure 13), as the sediment accumulated in the conductivity cell washes off upon ascent, and results in post-mission calibration coefficients that do not capture the salinity drift and are not representative of deployed conditions. Temperature and pressure, along with conductivity, are used to calculate potential temperature (**θ**) and density (**ρ**) adjusted to the nearest 1000 dbar-reference pressure, which is 6000 dbar at KEO. Salinity is also calculated from these values, using the methods of Fofonoff and Millard (1983). A standard 13-point Hanning filter was used to generate hourly data, and a boxcar filter created the daily averages.

Density and salinity are expected to be consistent between deployments, especially in density adjusted for pressure ($\sigma_{6000}$). Despite this expectation for year-to-year consistency in the deep ocean, the deep instruments at KEO have repeatedly experienced the fresh drift mentioned above (0.03 – 0.06 PSU), with initial deployment values near 34.69 PSU confirmed by comparison CTD casts. The deep instrument drift, attributed to sediment accumulation in the conductivity cell, propagates into an error in computed salinity and density, generating discontinuities between deployments. These deployment-to-deployment discontinuities were observed regardless of which calibrations were applied, and no post-processing method is known to effectively reduce the discontinuities.

### 3.3.5 Currents

Upward-looking point current meters were deployed at three depths on the KE016 mooring. The stated head depth differs from the actual current measurement depth, because the instruments require a blanking distance. Currents from the instruments deployed at 8.46, 16.46 and 36.46m measured velocities at 8, 16 and 36m, respectively. All current meters deployed on KE016 were Nortek Aquadopps, and no Aquadopp Profiler was deployed, although the profiler, first tested on KE015, will be featured on future deployments.

The current meters calculate the speed of sound, and internally apply sound velocity corrections to current measurements. During post processing, a correction for magnetic declination (-5.0°) is applied to the delayed-mode data. A thirteen-point Hanning filter is applied to the 10-minute resolution data to get hourly data, and a boxcar filter produces daily averaged values.

Since the KEO buoy could move about its watch circle, the current meters did not measure true currents. Using time-stamped data from the Flex system's GPS data, buoy velocity averages were generated. True currents were determined by adding calculated buoy motion to the measured current meter data.

Buoy motion was determined by first interpolating the acquired GPS positions onto a 10-minute grid (:05, :15, :25, etc.). Ten-minute mooring velocities corresponding to the current meter measurement intervals (:00, :10, :20, etc.) were then calculated using the haversine formula, to equate change in position over time to a mooring velocity. The calculated U and V mooring velocities used to correct the current meters are shown in Figure 14.

No flags were provided by the GPS systems, so data processors flagged the few acquired positions which placed the buoy outside the normal watch circle, but otherwise trusted the reasonable positions and calculated velocities. A few buoy-motion spikes occur when GPS timestamps are closely spaced, but short periods of high velocities are possible, so positions were not removed.

As mentioned in Section 2.3, the current meters experienced several failure modes associated with low batteries and ramifications from the instrument cascades. The 8m AQD data ended 12/22/2018 with a low battery, which is thought to have occurred prior to the instrument cascade based on pressure data. The 16m AQD short circuited, resulting in no data download, but realtime data exist through 3/31/2019. The final 36m AQD failed with a low battery on 7/10/2019, but downloaded in the lab after some internal wire repairs.

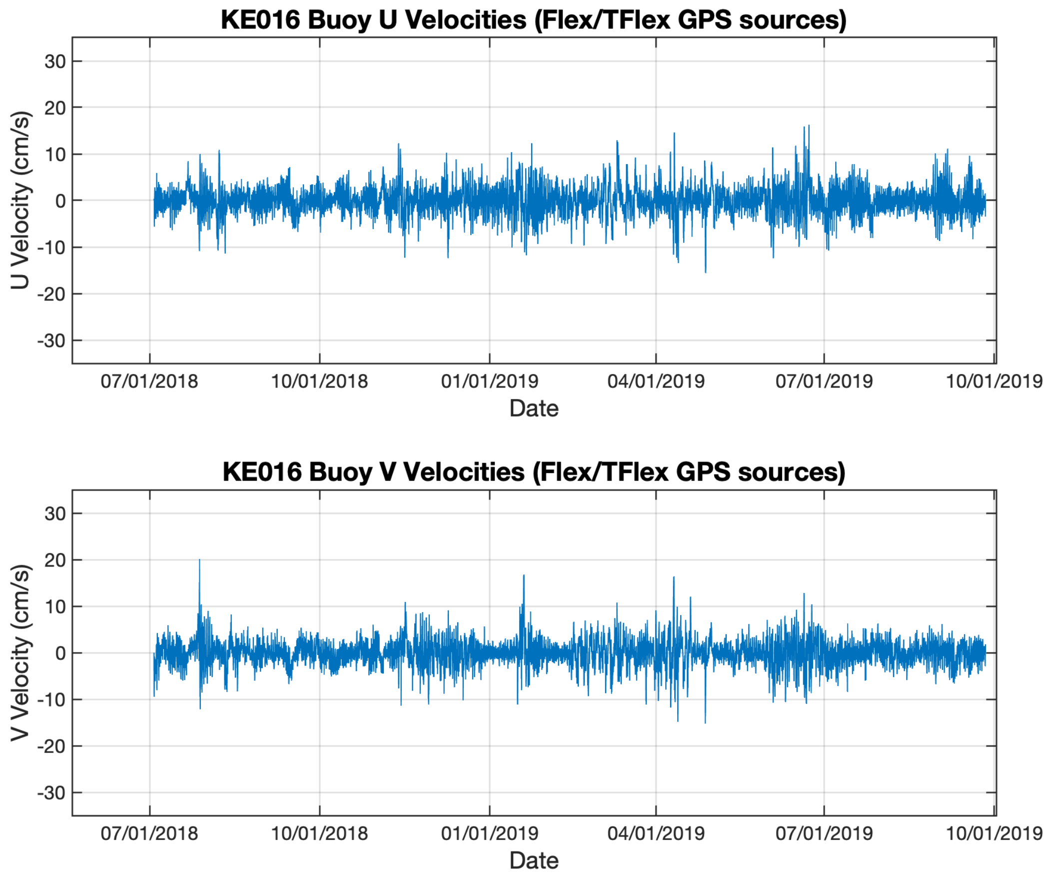

**Figure 14: KE016 buoy velocities used to correct currents.**

## 4.0 References

Anderson, N.D., K.A. Donohue, M.C. Honda, M.F. Cronin, and D. Zhang, 2020: Challenges of measuring abyssal temperature and salinity at the Kuroshio Extension Observatory, J. Atmos. Ocean. Tech., 37(11), 1999-2014.

Freitag, H.P., M.E. McCarty, C. Nosse, R. Lukas, M.J. McPhaden, and M.F. Cronin, 1999: COARE Seacat data: Calibrations and quality control procedures. NOAA Tech. Memo. ERL PMEL-115, 89 pp.

Fairall, C.W., P.O.G. Persson, E.F. Bradley, R.E. Payne, and S.P. Anderson, 1998: A new look at calibration and use of Eppley Precision Infrared Radiometers. Part I: Theory and Application. J. Atmos. Ocean. Tech., 15, 1229-1242.

Fofonoff, P., and R. C. Millard Jr., 1983: Algorithms for computation of fundamental properties of seawater, Tech. Pap. Mar. Sci., 44, 53 pp., Unesco, Paris.

Serra, Y.L., P.A'Hearn, H.P. Freitag, and M.J. McPhaden, 2001: ATLAS self-siphoning rain gauge error estimates. J. Atmos. Ocean. Tech., 18, 1989-2002.

## 5.0 Acknowledgements

N. Anderson (UW CICOES) processed the Flex/TFlex data on KE016. D. Dougherty (UW CICOES) is recognized for designing and generating the initial python files from which processing begins, and for the quality control of real-time data.

The OCS project office is grateful to the captain and crew of the M/V BLUEFIN and M/V KAIYO MARU #1, who made the deployment and recovery operations possible. P. Berk and T. Nesseth deployed the KE016 mooring and P. Berk, B. Higley, and N. Anderson (all of UW CICOES) participated in the recovery cruise.

This work was supported by NOAA's Global Ocean Monitoring and Observing Program (FundRef number 100018302).

## 6.0 Contact Information

For more information about this mooring and data set, please contact:

Dr. Meghan Cronin
meghan.f.cronin@noaa.gov

NOAA/PMEL/OCS
7600 Sand Point Way NE
Seattle, WA 98115

## APPENDIX A: Description of Data Quality Flags

Instrumentation recovered in working condition is returned to PMEL for post-recovery calibration before being reused on future deployments. The resultant calibration coefficients are compared to the pre-deployment coefficients, and measurements are assigned quality indices based on drift, using the following criteria:

Q0 - No Sensor, or Datum Missing.

Q1 - Highest Quality. Pre/post-deployment calibrations agree to within sensor specifications. In most cases, only pre-deployment calibrations have been applied.

Q2 - Default Quality. Pre-deployment calibrations only or post-recovery calibrations only applied. Default value for sensors presently deployed and for sensors which were not recovered or not calibratable when recovered, or for which pre-deployment calibrations have been determined to be invalid.

Q3 - Adjusted Data. Pre/post calibrations differ, or original data do not agree with other data sources (e.g., other in situ data or climatology), or original data are noisy. Data have been adjusted in an attempt to reduce the error.

Q4 - Lower Quality. Pre/post calibrations differ, or data do not agree with other data sources (e.g., other in situ data or climatology), or data are noisy. Data could not be confidently adjusted to correct for error.

Q5 - Sensor, Instrument or Data System Failed.

For data provided in OceanSITES format, the standard GTMBA quality flags described above are mapped to the different OceanSITES quality flags shown below:

Q0 - No QC Performed.
Q1 - Good Data. (GTMBA Q1, Q2)
Q2 - Probably Good Data. (GTMBA Q3, Q4)
Q3 - Bad Data that are Potentially Correctable.
Q4 - Bad Data. (GTMBA Q5)
Q5 - Value Changed.
Q6 - Not Used.
Q7 - Nominal Value.
Q8 - Interpolated Value.
Q9 - Missing Value. (GTMBA Q0)

# APPENDIX B: Primary Instrument High Resolution Data Plots

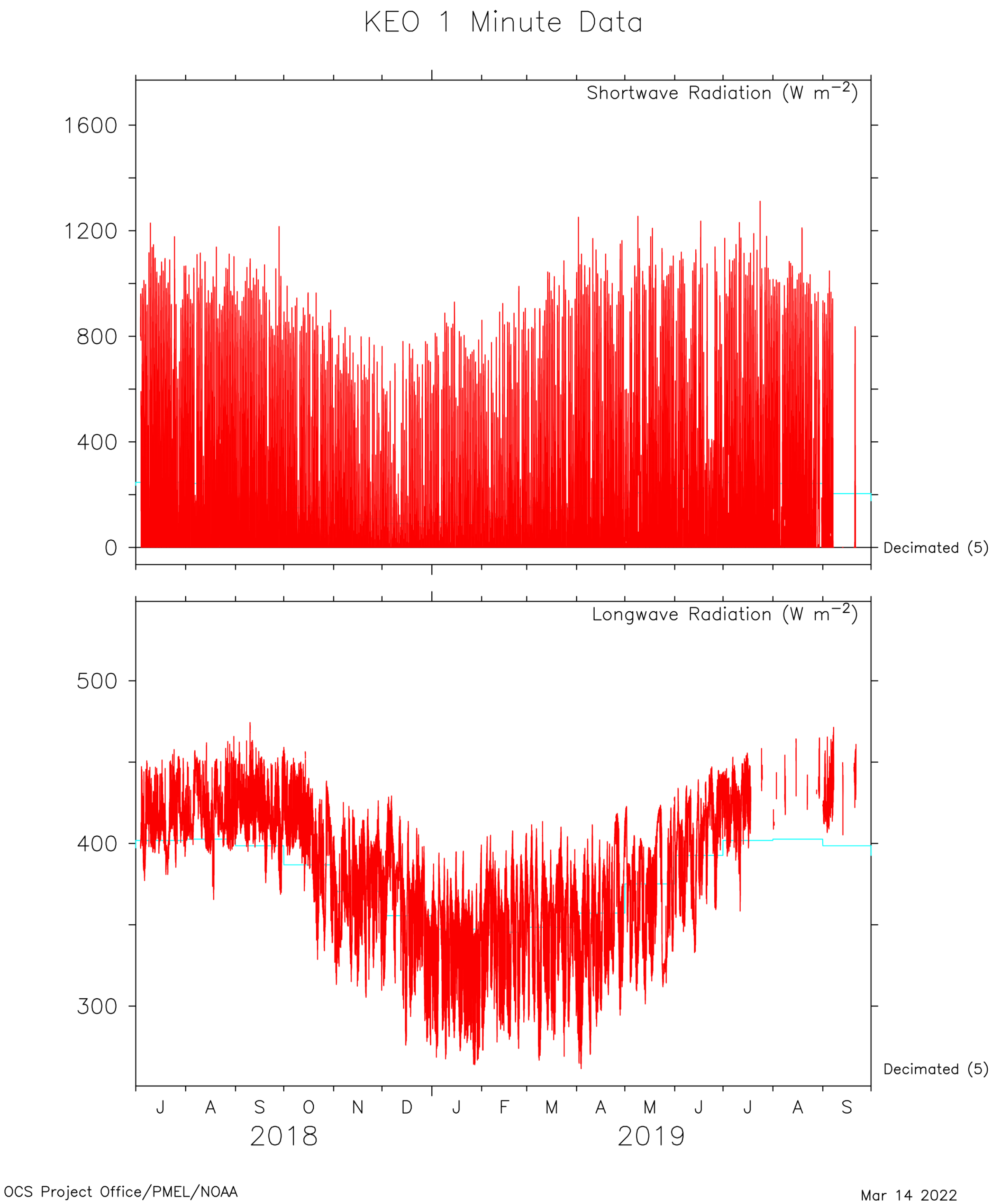


**Figure B 1: KE016 primary shortwave and longwave radiation data at 1-min resolution (TFlex).**

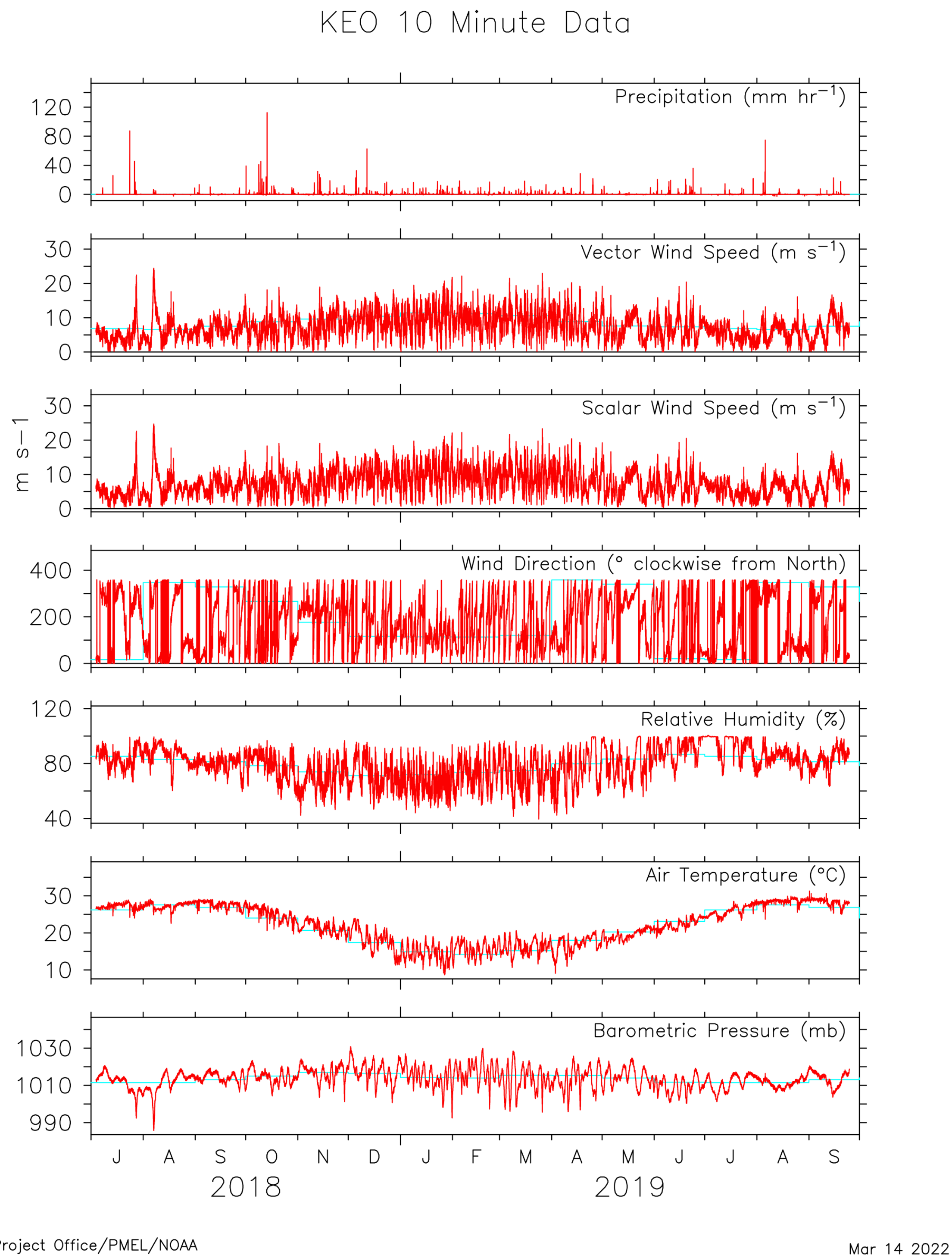


**Figure B 2: KE016 primary meteorological data at 10-min resolution. All data are from TFlex, except winds.**

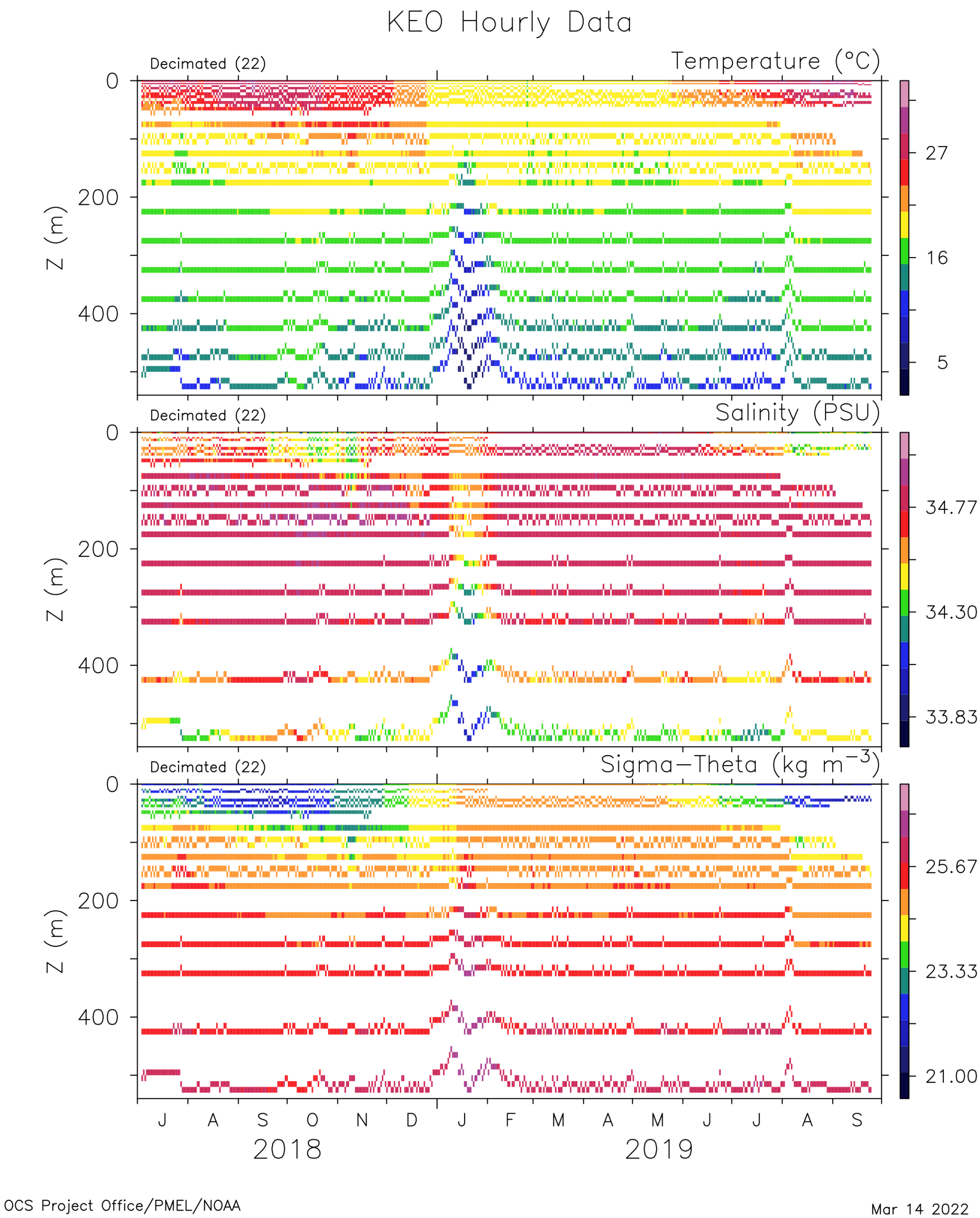


**Figure B 3: KE016 subsurface temperature, salinity, and density at hourly resolution (decimated).**

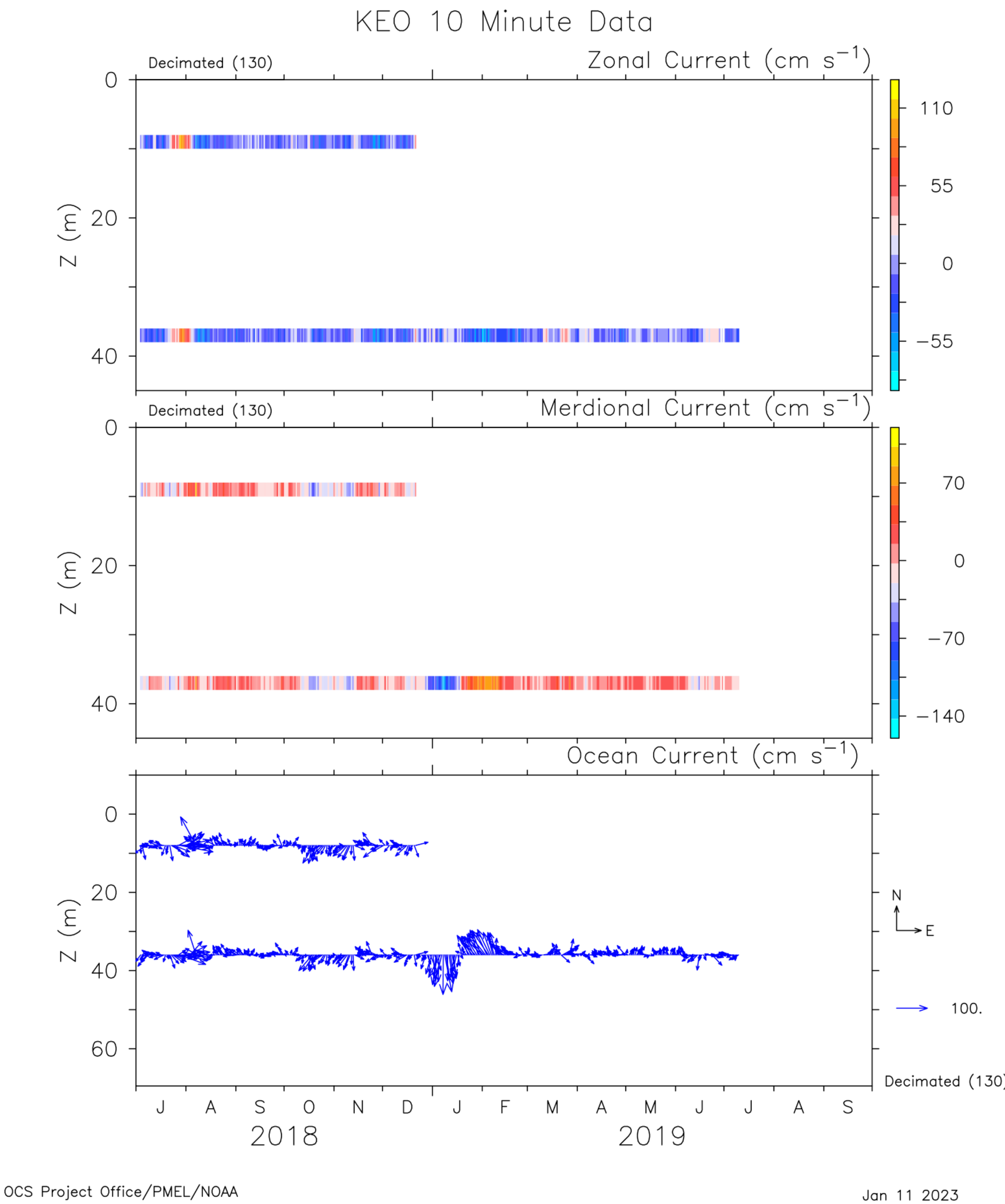


**Figure B 4: Zonal and meridional current meter data (decimated) from KE016. Note that 16m Aquadopp data are available in realtime (hourly/daily resolution), but the instrument flooded, so no high-resolution data are available.**

# APPENDIX C: Secondary Instrument High Resolution Data Plots

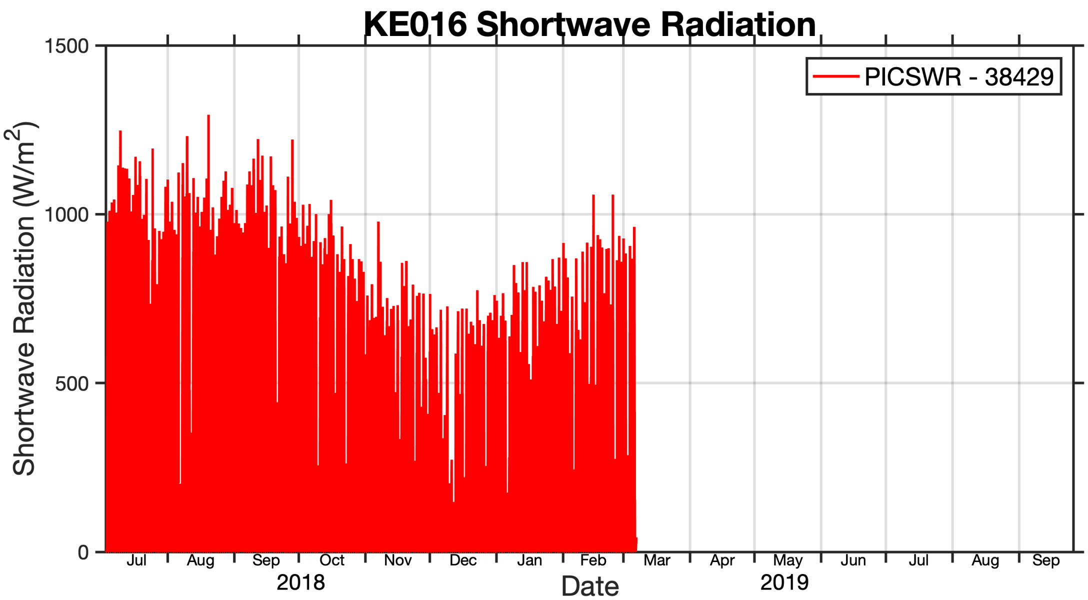


**Figure C 1: Secondary (Flex Eppley PSP) shortwave radiation sensor. The Flex system's power consumption was high by mid-deployment, so many surface sensors were shut off in March 2019 to preserve realtime telemetry of subsurface data.**

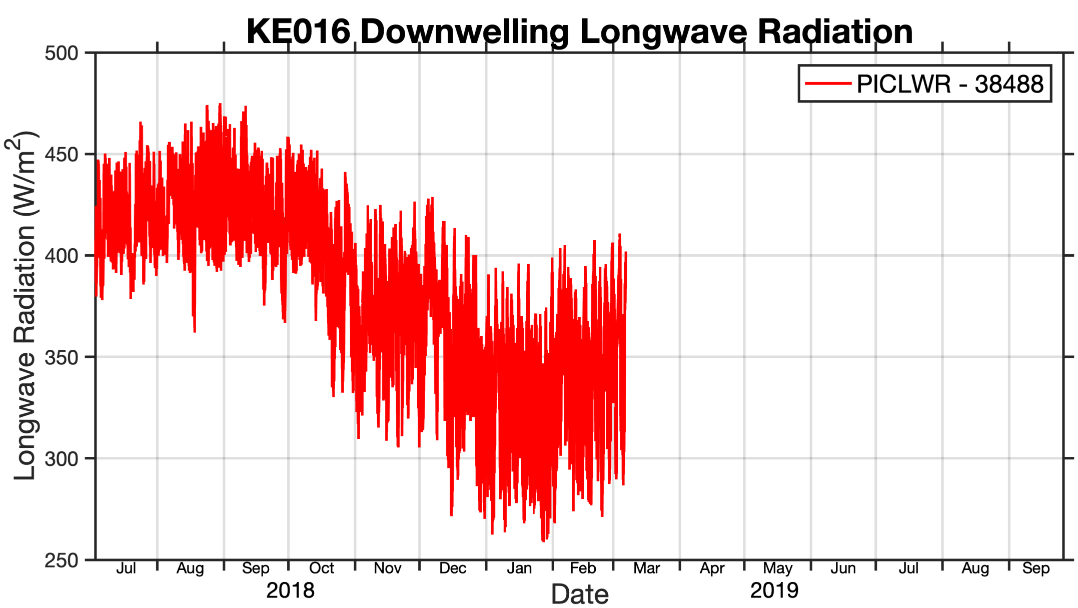


**Figure C 2: Secondary (Flex Eppley PIR) longwave radiation sensor.**

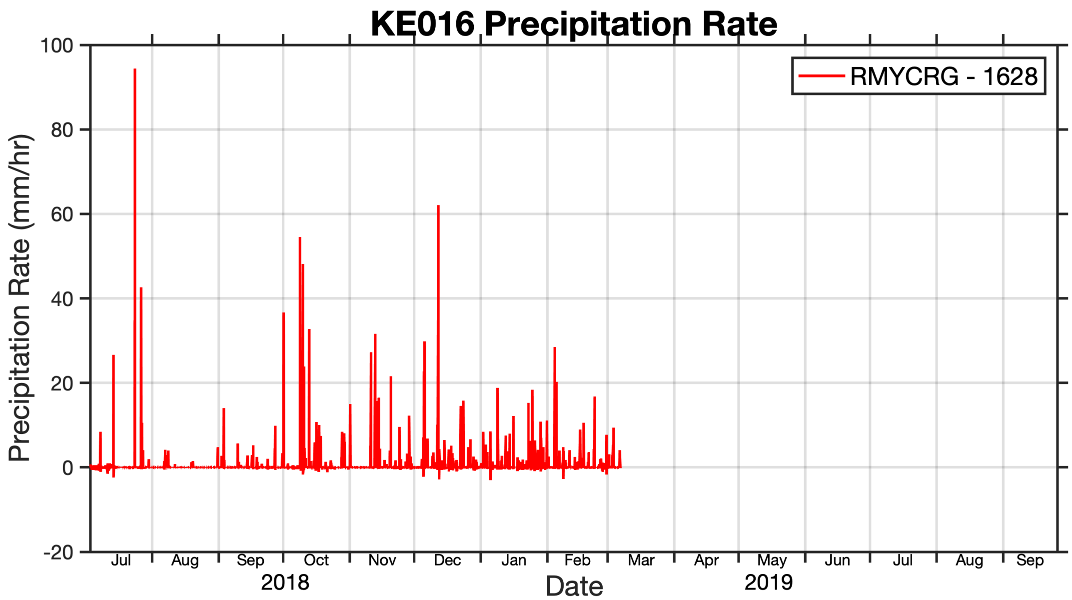


**Figure C 3: Secondary (Flex RM Young) rain sensor. The high spikes are likely real, as several typhoons were documented during this deployment.**

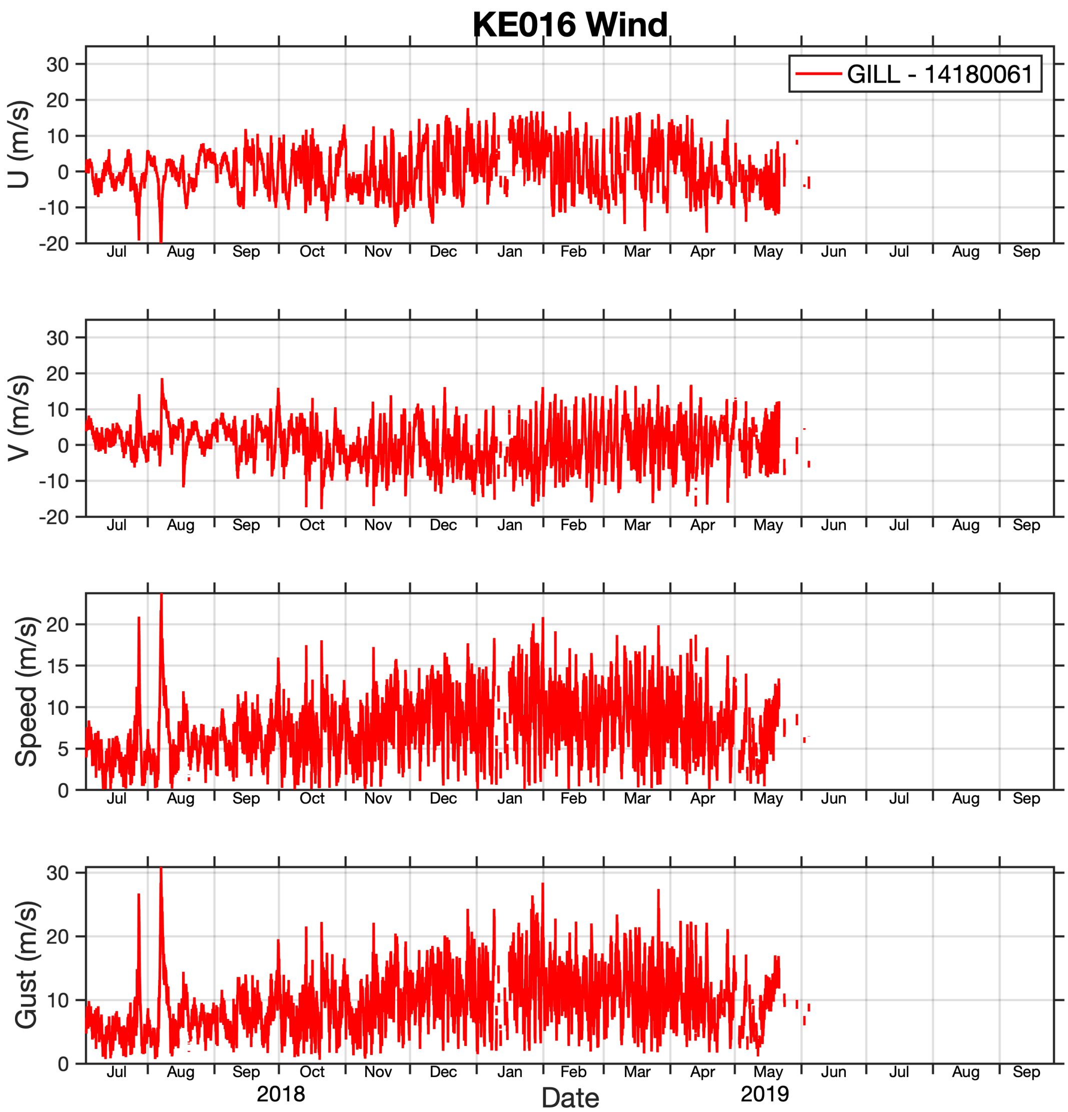


Figure C 4: Secondary (TFlex Gill) wind sensor.

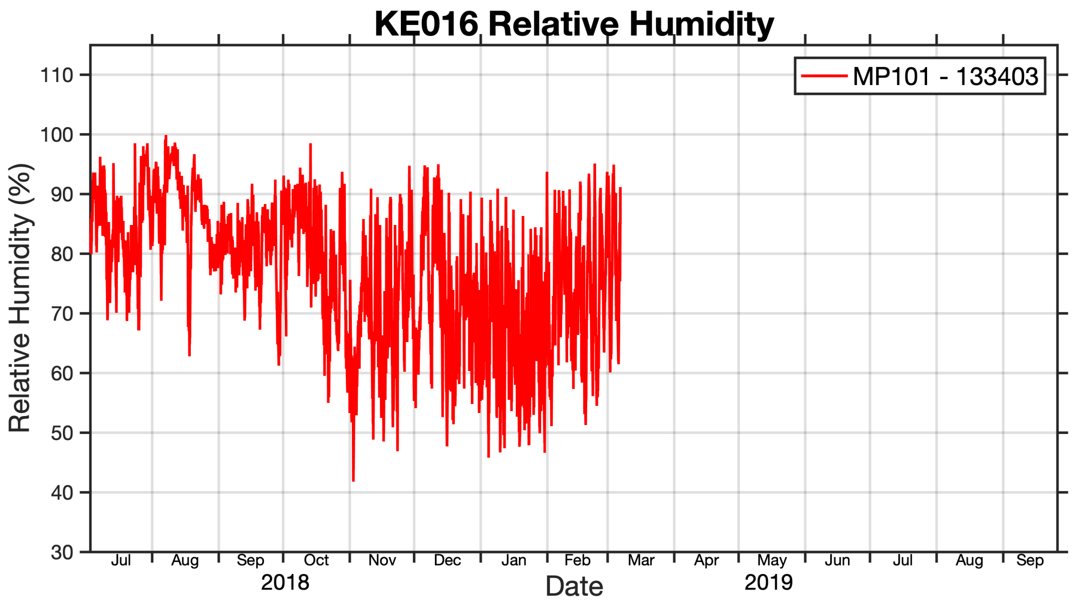


**Figure C 5: Secondary (Flex MP101) relative humidity sensor.**

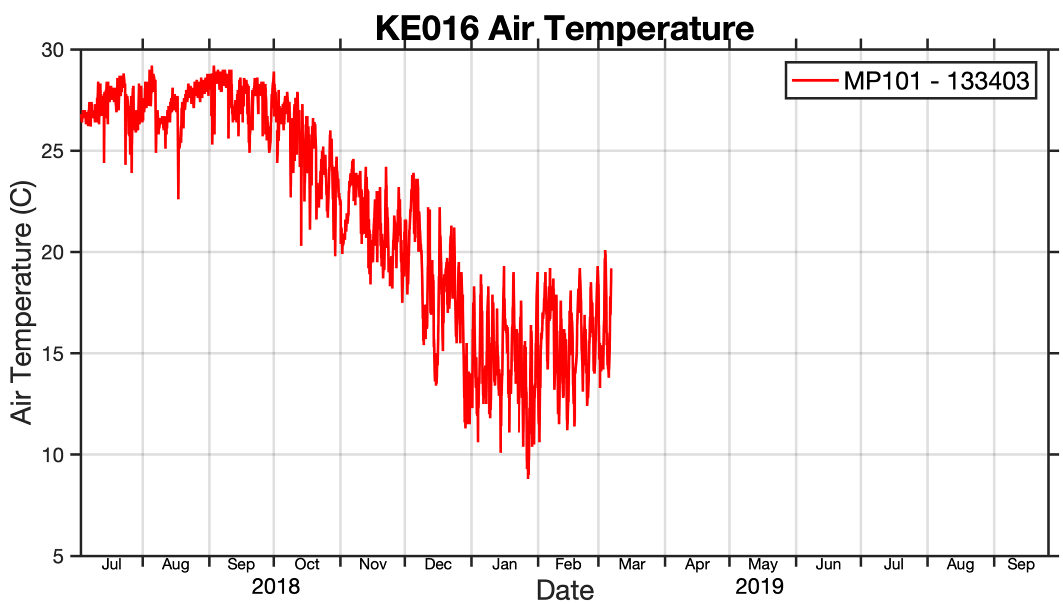


**Figure C 6: Secondary (Flex MP101) air temperature sensor.**

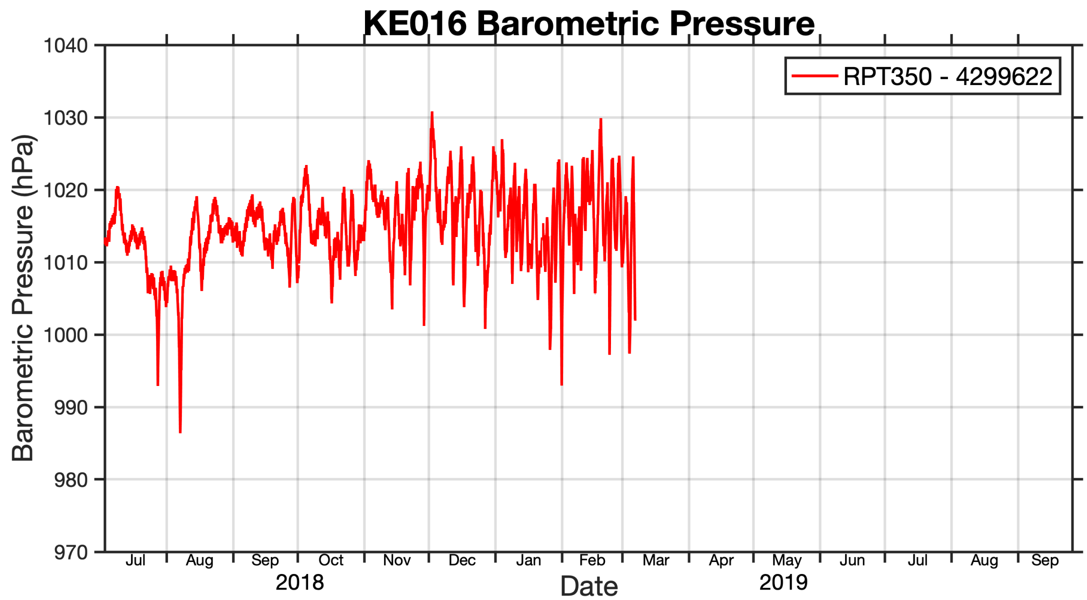


Figure C 7: Secondary (Flex Druck) barometric pressure sensor.

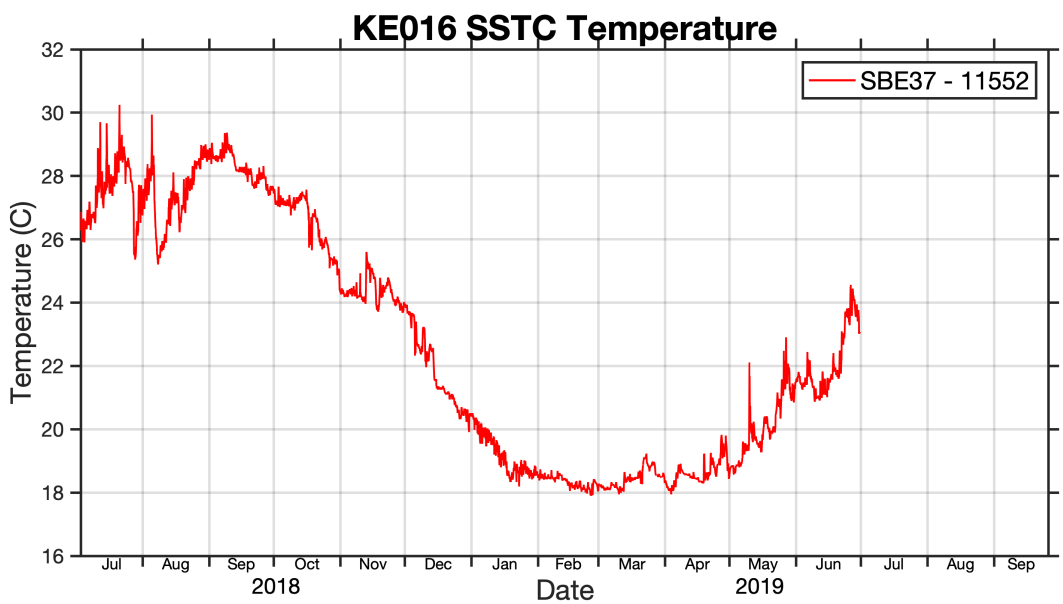


Figure C 8: Secondary (TFlex) SSTC temperature.

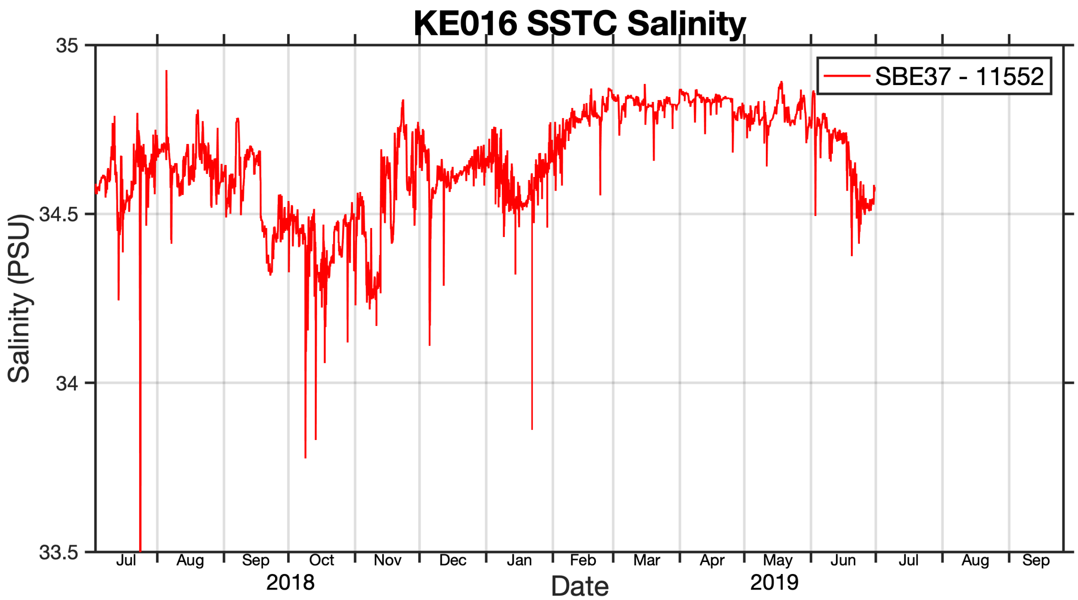


**Figure C 9: Secondary (TFlex) SSTC salinity. The fresh spikes were allowed to pass quality control, as typhoon and/or storm passage can produce a fresh lens of water at the surface.**

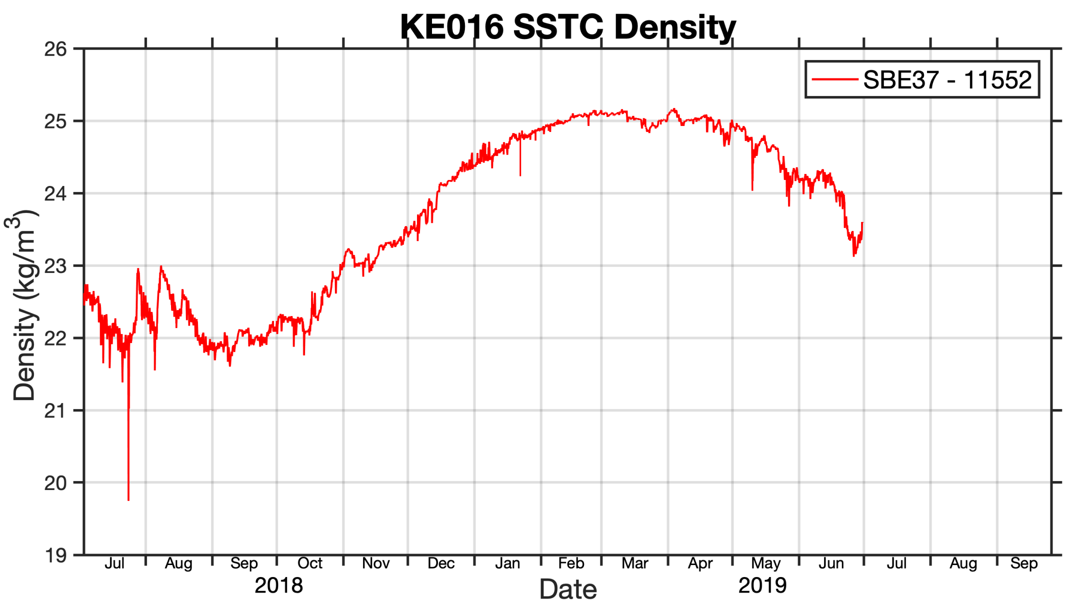


**Figure C 10: Secondary (TFlex) SSTC density.**